ICDD Working Papers | Paper No. 26 | Sept. 2019

ICDD

Anjum Munir & Oliver Hensel

Solar Thermal Energy Storage System

using phase change material for uninterrupted on-farm agricultural processing and value addition

The International Center for Development and Decent Work

Anjum Munir is an Associate Professor and Chairman in the Department of Energy Systems Engineering, Faculty of Agricultural Engineering and Technology, University of Agriculture Faisalabad, Pakistan. He holds a PhD degree in Agricultural and Biosystems Engineering from University of Kassel, Germany. His main focused research areas are solar thermal and photovoltaic systems, bioenergy, energy conservation and auditing measures, energy storage. He has launched new B.Sc. and M.Sc. degree programs on Energy Systems Engineering accredited from Higher Education Commission (HEC) and Pakistan Engineering Council (PEC). Dr. Munir is engaged in teaching and research related to the subjects of energy resources and utilization, engineering thermodynamics, boiler engineering and power plants, I.C. engines, solar energy, HVAC, among others. He has published more than 60 scientific publications. He has also developed eight solar based technologies for value addition of agricultural product. Dr. Munir is an approved PhD supervisor from Higher Education Commission (HEC) Pakistan and has supervised three PhDs students and 45 MS students as major supervisor and 39 as member of supervisory committee during his teaching tenure. He has successfully completed more than 20 need based research projects on solar and bioenergy. He has provided consultancy services as a team leader to the Government of Punjab and has installed more 2300 solar drip irrigation systems in the whole Punjab Province of Pakistan for energy and water conservation. Dr. Munir has submitted four patents on innovative solar based technologies. He has won four consecutive times "Research Productivity Awards" from the Ministry of Science and Technology, Government of Pakistan and is included in top ranked list of "Productive Scientists of the country" within the discipline of Engineering and Technology.

Oliver Hensel is full professor since 2004 and the head of the section of Agricultural and Biosystems Engineering at the Faculty of Organic Agricultural Sciences at the University of Kassel. His teaching and research focus is on technology of plant production as well as a vast set of topics such as technology of animal husbandry, processing, drying, storage, engines, alternative and renewable energy, environmental technology, landscape conservation, electronic- and database use, automation of agricultural processes, agricultural engineering, ergonomic analysis, accident prevention, irrigation, and land drainage in industrialized and developing countries.

Contact Address
Prof. Dr. Christoph Scherrer
ICDD – University of Kassel, Germany
Mailing address: Mönchebergstr. 19, D-34109 Kassel
Visitors' address: Kleine Rosenstr. 3, D-34117 Kassel
Contact: felmeden@icdd.uni-kassel.de

Design / Layout: Nina Sangenstedt, gestaltvoll.de

ICDD Working Papers
ISBN: 978-3-7376-0634-9 (print)
ISBN: 978-3-7376-0635-6 (e-book)
DOI: http://dx.medra.org/10.19211/KUP9783737606356

First published 09/2019 in Kassel, Germany

Publishing House:
kassel university press GmbH
www.upress.uni-kassel.de

kassel university press

Anjum Munir & Oliver Hensel

Solar Thermal Energy Storage System

using phase change material for uninterrupted on-farm agricultural processing and value addition

Contents

Abstract

Thermal energy storage technologies are gaining attention nowadays for uninterrupted supply of solar power in off-sunshine hours. An indigenized solar phase change material (PCM) system was developed and performance evaluated in the current study to efficiently store solar thermal power using a latent heat storage approach, which can be utilized in any subsequent decentralized food processing application. A 2.5 m^2 laying Scheffler reflector is used to precisely focus the incoming direct normal irradiance (DNI) on a casted aluminum heat receiver (220 mm diameter) from where this concentrated heat energy is absorbed and conducted to the PCM unit by the flow of thermal oil (Fragoltherm-32 thermo-oil). During the circulation around PCM pipes inside the PCM unit, thermal oil discharges heat energy to the PCM, which undergoes change of phase from solid to liquid. Computational fluid dynamics (CFD) analysis of the PCM unit were also performed according to the actual boundary conditions, which gave satisfactory results in terms of temperature and velocity distribution. With an average DNI of 781 W/m^2, the highest temperature of the receiver surface during the trials was observed at about 155 C that produces thermal oil at 110°C inside the receiver and around 48°C of PCM in the PCM unit. The heat energy losses per unit time (W) due to the lack of reflectivity from the Scheffler reflector, out-of-focus radiations at the targeted area, absorptivity of heat receiver, piping system losses, and cylinder losses (in the form of conduction, convection, and radiations using 50 mm insulation thickness) were found to be 110 W (10%), 99 W (9%), 89 W (8%), 128 W (12%), 161 W (15%), and 89 W (8%), respectively. These findings of CFD analysis and mathematical modeling were also consistent with real-time data, which was logged through an online Control and Monitoring Interface portal. The final energy available to the PCM was 414W with an overall system efficiency of 38%, which can be improved by decreasing thermal losses of the system and using other PCM materials.

Key words: *Latent heat storage, Mannitol, Computational fluid dynamics, Scheffler reflector, Solar heat receiver.*

1 Introduction

The global food loss along supply chain (harvest to consumption) is estimated to be 30%, that is, around 1 trillion USD annually (FAO, 2013). Food security is directly correlated to industrialization which needs heavy energy inputs. The agricultural processing sector, in particular, dominantly consumes about 30% of the total global energy production and emits around 10 billion Greenhouse gases (GHGs) (CO_2 equivalent) per year (FAO, 2011). Carbon dioxide (CO_2) and methane (CH_4) concentrations in the atmosphere are found to have increased significantly by 31% and 149%, respectively, since the beginning of the industrial revolution in the 1750s (Neftel et al., 1985; Akorede et al., 2012). The immense use of fossil fuels, as the primary energy source, has created a polluted environment; hence, this demands serious attention. The expanding industrialization needs to shift to renewable energy resources. Industrial processes operating between ambient to 180°C utilizes directly 24% industrial heat which can be availed through appropriate solar concentrators (Garg and Prakash, 2006). In medium to high temperature range (60°C–280°C), most processes in the industries like drying, pasteurizing, sterilizing, hydrolyzing, extraction, etc. (Kalogirou, 2003) can also be performed by applying solar thermal energy. Solar heat concentration is the prominent technology being developed in various countries since the last few decades. Efforts are in process to apply solar energy to agricultural processing. Currently, solar collectors are widely used for drying and water heating whereas this technology can also be applied on perishable food products for farm gate processing (EESI, 2011). By introducing innovative solar thermal collectors, small-scale agricultural processing industries can be promoted which will contribute towards sustainable rural development, especially in the tropical regions.

Concentrating solar power (CSP) provides a magnificent platform to meet the heat demand of industrial thermal processes. Among the available solar concentrating technologies, Scheffler-fixed focus concentrator is the best suitable option for generating heat energy in medium to high temperature range with a variety of reflector sizes ranging from 2 m^2 to 60 m^2 (Scheffler et al., 2006; Panchal et al., 2018). The versatility of Scheffler reflector is to keep the focus fixed on the heat receiver which provides a uniform temperature distribution on the heat receiver's surface. The essential feature of a heat receiver is to absorb the maximum amount of concentrated solar energy and transfer it to the heat transfer fluid (HTF) as heat energy which can be further utilized in any subsequent process (Kumar and Reddy, 2007). Scheffler reflectors up to 50 m^2 were successfully tested for the generation of about 700°C which shows tremendous potential of this technology in almost all types of high-temperature-range processing industries (Scheffler et al.,

2006). Up till now, the Scheffler reflectors are efficaciously employed to produce heat energy for domestic water heating (Patil et al., 2011; Akhade and Patil, 2015), cooking applications (Chandak and Somani, 2009; Dafle and Shinde, 2012), steam generation (Sudhir and Feroz, 2016), distillation (Afzal et al., 2017), desalination (Chandrashekara and Yadav, 2017), coffee making (Kamboj and Yadav, 2017), ceramic processing (Acharya and Chandak, 2013), and electricity generation (Ruelas et al., 2015).

Besides the tremendous scope of solar energy, one major limitation is its availability during day time only and the dependency on weather fluctuations and sunshine hours which varies additionally in different seasons. Supplementary energy derived from conventional resources is generally provided in order to achieve continuous operation which adds both cost and complexity to the system. Thermal storage devices can therefore provide a good alternate solution to address this problem as they can store the extra energy all through day time which can be utilized during off-sunshine hours (Ahmet et al., 2008). It is estimated that about 7.5 % of total energy that is consumed in the European Union (EU) in a single year can be saved by utilizing thermal energy storage systems (Arce et al., 2011). For the last three decades, there has been a growing interest in latent heat thermal storage (LHTS) technique which is proved to be a better option over sensible heat storage (Jegadheeswaran, 2010) as LHTS offers high density energy storage and temperature fluctuation between storage and release of energy as compared to sensible heat storage (Farid et al., 2004). In LHTS units, phase change materials (PCM) are used which undergo change of phase (solid to liquid and vice versa) during the energy transfer process. The key feature of LHTS systems is that the equivalent amount of heat energy stored in PCM during melting can be retrieved during solidification (Castell et al., 2008). A variety of PCMs are available according to design-specific configurations of the system and their applications in various engineering fields (Zalba et al., 2003; Farid et al., 2004; Sharma and Sagara, 2005; Kenisarin and Mahkamoy, 2007).

Currently, solar energy is successfully utilized for steam generation and various cooking applications. Using of Scheffler reflector with a PCM heat storage system is a novel and promising area of research for the utilization of solar thermal energy in medium to high temperature range. By keeping all facts in view, the study has been initiated at the Solar and Irrigation Demonstration Plant, Witzenhausen, Germany to develop a decentralized solar PCM system for the storage of heat energy which can be utilized after sun hours or during cloudy weather.

2 Review of Literature

Energy indemnity has significant importance in the escalating industrialized world. Meanwhile, immense use of depleting fossil fuel power generation is negatively affecting the global environment and creating a huge challenge for food security. This chapter briefly describes an overview of food losses, role of industries in global warming, scope of CSP in agricultural processing, and existing solar PCM technologies.

2.1 Food Security in the Industrialized World

The world is predicted to be populated around 9.1 billion by 2050 which will require about 70 % increased food availability especially in developing countries, where urban population is increasing steadily and creating lengthy and complex food supply chain (FAO, 2009). Currently, the global food losses along supply chain (harvest to consumption) are estimated to be 30 % valuing around 1 trillion USD annually (FAO, 2011). Food losses show different patterns in different regions as depicted in Fig. 2.1. The quality-based food losses are dominant in industrialized countries whereas in developing countries, food scarcity risk is more due to higher percentage of post-harvest and processing losses (14 %–21 %) than developed ones (< 2 %) (FAO, 2011). There are many factors including inadequate energy resources and their utilization, conventional agriculture practices, lack of processing facilities, underdeveloped infrastructure, and limited access to international markets which cause food loss in the food supply chain in these countries (FAO 2009; Rezaei and Liu, 2017). Food losses also adversely affect food security, economic and environment values along with the wastage of energy resources used during food loss which accounts for an annual 3.3 gigatons (Gt) of GHG emissions (CO_2 equivalent). With these huge emissions, food wastage is ranked world's third largest GHG emitter after China and the United States (FAO, 2013).

Figure 2.1: Percentage of losses for fruits and vegetables in different regions at different stages of processing

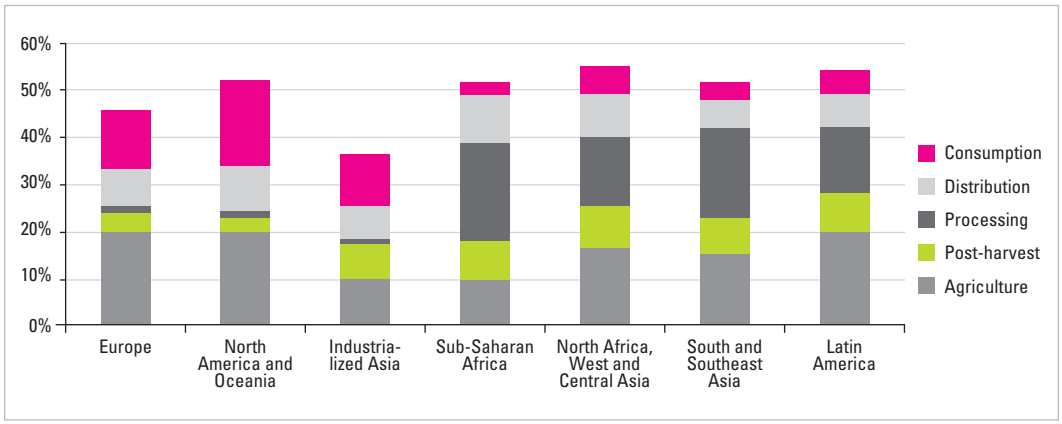

Source: Rezaei and Liu, 2017

On the other hand, after the industrial revolution started in the mid-seventeenth century, GHG emissions have risen tremendously due to anthropogenic activities. The global emission of CO_2 has increased from 2 to 36 Gt in the last century (Fig. 2.2) in which energy sector emissions contributed up to 72 % (World Resources Institute, 2017). These GHG emissions resulted in an increase of 1°C in the overall globe temperature (Quaschning, 2010) out of which 0.74 + 0.18°C has increased just between 1906 and 2005 (Barker et al., 2007).

Figure 2.2: Annual Global CO_2 emission by region

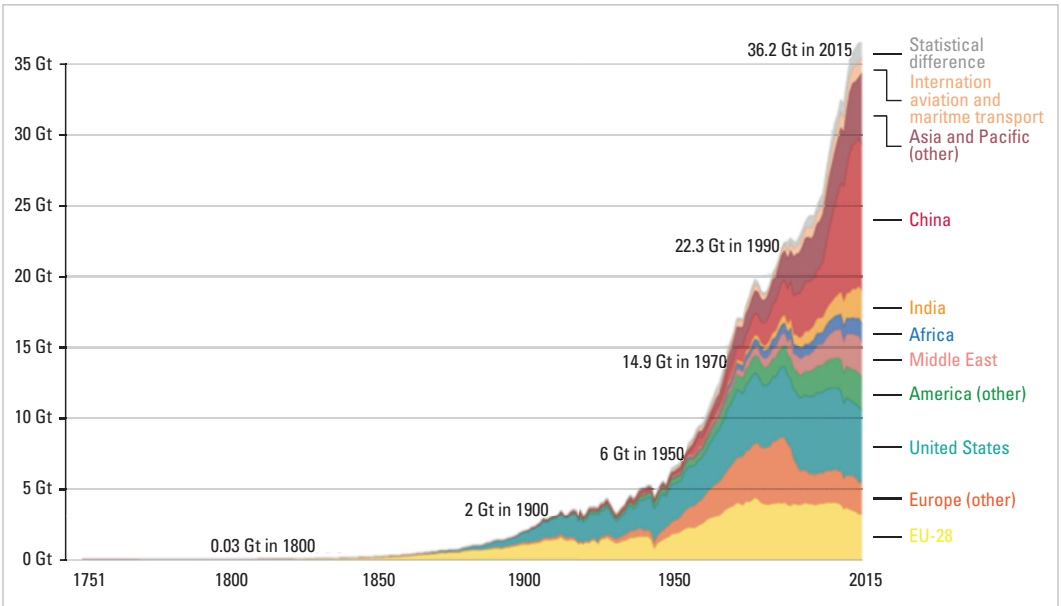

Source: Le Quéré et al., 2016.

The necessity of fossil fuels can never be overemphasized in the modern world, as they are extensively used for energy generation. The fossil fuel-based power plants used for the energy generation are the most notorious emitters of GHGs. In 2016, fossil fuel alone fulfilled 85 % of the world primary energy demand (Tverberg, 2018) and their use is expected to grow in absolute terms over the next 20–30 years. Fossil fuels are considered as non-renewable resources of energy because they are formed in millions of years by the anaerobic decomposition of buried dead organism and being utilized at a faster rate. By depleting the reserves of fossil fuels at the same rate, the world will be facing a challenging situation having insufficient non-renewable energy resources at the end of the twenty-first century (Höök and Xu, 2013).

Food security is directly correlated to industrialization which needs heavy energy inputs. Particularly the agricultural processing sector, which dominantly consumes about 30 % of total global energy production and emits GHGs around 10 billion (CO_2 equivalent) per year (FAO, 2011), needs to be addressed well to tackle food scarcity and climate change issues in an efficient, integrated and sustainable way by exploiting alternate reserves of nature i.e., renewable energies.

2.2 Scope of CSP in the Processing Sector

The industrial sector shows a tremendous scope of CSP as most of the industrial processes require heat energy in 80°C–240°C temperature range (Kalogirou, 2003). Globally, China, Malaysia, Turkey, United States (US), and Germany utilize 70 %, 45 %, 35 %, 33 %, and 27 %, respectively, of their total energy production directly in industrial processing (Abdelaziz et al., 2011; Lauterbach et al., 2012). Nature has blessed mankind with enormous potential of renewable energy resources and solar energy is one of them. Generally, solar energy is considered for electrical power generation, but it also may be applied in agricultural as well as industrial processes for heat generation through various CSP technologies (IEA, 2011). Surprisingly, the conversion efficiency (ratio of energy produced by the collector to the energy of the sunlight) of a solar thermal energy-based system (70 %) is reported much higher than the electricity producing photovoltaic panels (17 %) (Jaisankar et al., 2011).

The International Energy Agency (IEA) avowed the CSP as a very promising but untapped technology which can be applied to industrial applications (IEA, 2008). In 2016, the total global installed capacity of CSP has been grown to 4.8 GW in which 80 % shares are held by the US and Spain. Accompanying to this escalation in CSP installation, the shifting trend of CSP technologies towards developing countries has also been seen from 2015 which further continues in 2016 with an investment of 57.5 billion USD in solar-based technologies. CSP technologies are getting more economic attraction day by day as their costs have declined by 18 % from 2010 to 2016 which sets up the levelized cost of energy (LCOE) to USD 0.27/ kWh (REN21, 2017). The LCOE of CSP for different regions of the world is given in Fig. 2.3.

Figure 2.3: LCOE for CSP in 2016

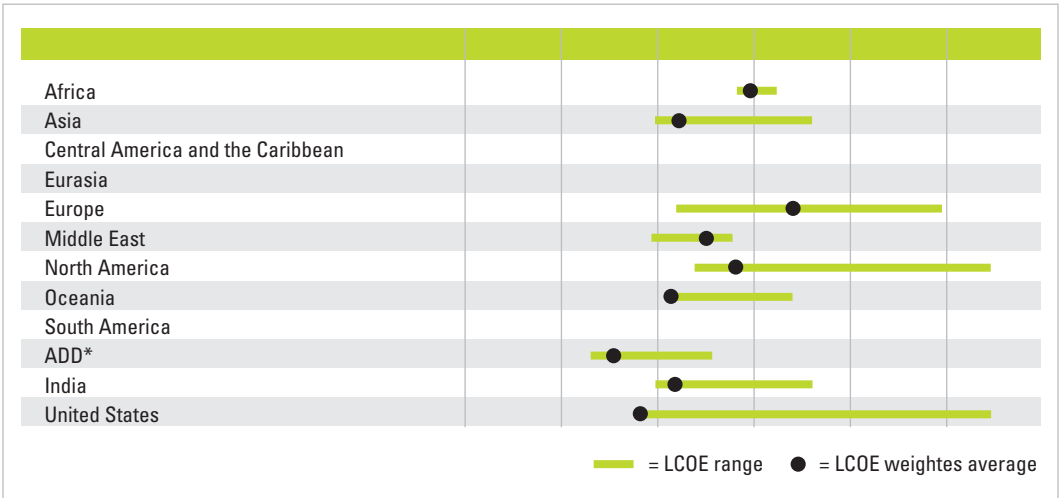

Source: REN21, 2017

2.3 Scheffler Reflector

In the past decades, many technological developments have been made for the utilization of solar energy in heat generation such as linear Fresnel (line focus), parabolic trough (line focus), heliostat field and parabolic dish (point focus each) but are rarely employed in industries due to focus is not fixed and tracking problems exists in them (EESI, 2011). Among the available concentrating solar collectors, there is a versatile elliptical concentrator i.e., Scheffler fixed focus concentrator, which not only provides a precise automatic sun tracking but also a fixed focus away from the path of incident beam radiations (Scheffler et al., 2006). These reflectors are equipped with a daily tracking (automatic) as well as seasonal tracking system (manual/automatic) to give a fixed focus throughout the year even with the changing solar declination angle. Scheffler reflector also offers an economically viable solution to meet the heat requirements of post-harvest processing operations for decentralized applications in far-flung areas, where there is no availability of fossil fuels or not even connections to conventional electric grid system. It also provides options to set the reflector in a standing position or in a laying position rotating along the same axis of rotation. For standing reflectors, the targeted focus is just near the ground level whereas in case of laying reflectors, the focus point is well above the ground level. The laying reflectors are useful for cooking purposes because they eliminate the use of secondary reflector and provide direct focus at the bottom of the heating container (Scheffler et al., 2006). A heat receiver can also be used to supply the high temperature heat to utilization end. It absorbs the heat energy from the focus point and transfers it to the HTF which delivers the absorbed energy to any useful process (Kumar and Reddy, 2007).

2.4 PCM Heat Storage

PCM-based LHTS systems offers a suitable solution to cover up the gap between energy source and demand, if the source is intermittent and time dependent like solar thermal energy (Jegadheeswaran, 2010). Solar thermal energy can be stored by using the latent heat of a PCM. PCM absorbs the excessive energy almost at constant temperature during high radiation periods which cause PCM to change its phase such as from liquid to gas or from solid to liquid. As the phase change chemical reaction is totally reversible, when low intensity of solar radiation decreases the input temperature, the stored energy in PCM is discharged and the PCM used for storage gains its initial form. In this way, PCM present high latent heat storage; moreover, a small volume of PCM is required as the melt and solidification are done at nearly constant temperature (Bennamoun, 2013). Selection of PCM is of paramount importance for the successful storage and retrieval of thermal energy and long-term reliability of the system. An ideal PCM should have good thermal conductivity and large latent heat. Moreover, it should be chemically stable, non-toxic and non-corrosive in nature (Farid et al., 2004). Sharma et al. (2009) and Bal et al. (2010) have presented a comprehensive work related to the classification of various PCMs, classified as inorganic (salt hydrates, metallics), organic (paraffins, non-paraffins) and eutectics materials with the detail of several physical properties such as latent heat, melting and freezing point range, and heat of fusion. Farid et al. (2004) and Zalba et al. (2003) also reported comprehensive details of various PCMs and their applications like drying, space and water heating. Accordingly, a lot of research work has been reported on the study of LHTS thermal behavior in many fields of agricultural processing e.g., drying, steam generation, etc. (Sharma and Sagara, 2005; Kenisarin and Mahkamoy, 2007).

The above-cited literature reveals that the world needs to be shifted from conventional fossil-fuel based sources of energy to renewable energy resources to avoid future food scarcity and global warming issues. Scheffler reflectors provide a better option for medium to high temperature range processing and emphasis should be made to use PCM-based storage systems in combination of these reflectors for enhanced utilization of CSP.

3 Materials and Methods

The study is conducted to develop a decentralized system to utilize concentrated solar power after sunshine hours with a suitable PCM heat storage system, which is installed at the solar and irrigation demonstration plant at Witzenhausen (51°20'32"N 9°51'28"E), Germany. The PCM technology is a practical and adoptable solution in rural areas for various operations like cooking, drying, space heating, etc. The present study is focused to fabricate a solar heat storage system with PCM from which the excessive stored energy can be utilized during off sunshine hours. The developed system comprised a laying Scheffler reflector (2.5 m^2 surface area), heat receiver (220mm in diameter), PCM heat storage and a thermal oil reservoir to collect the utilizable heat energy coming from PCM. The schematic diagram and working principle of the solar PCM system is shown in Fig. 3.1.

Figure 3.1: Schematic diagram of solar PCM system

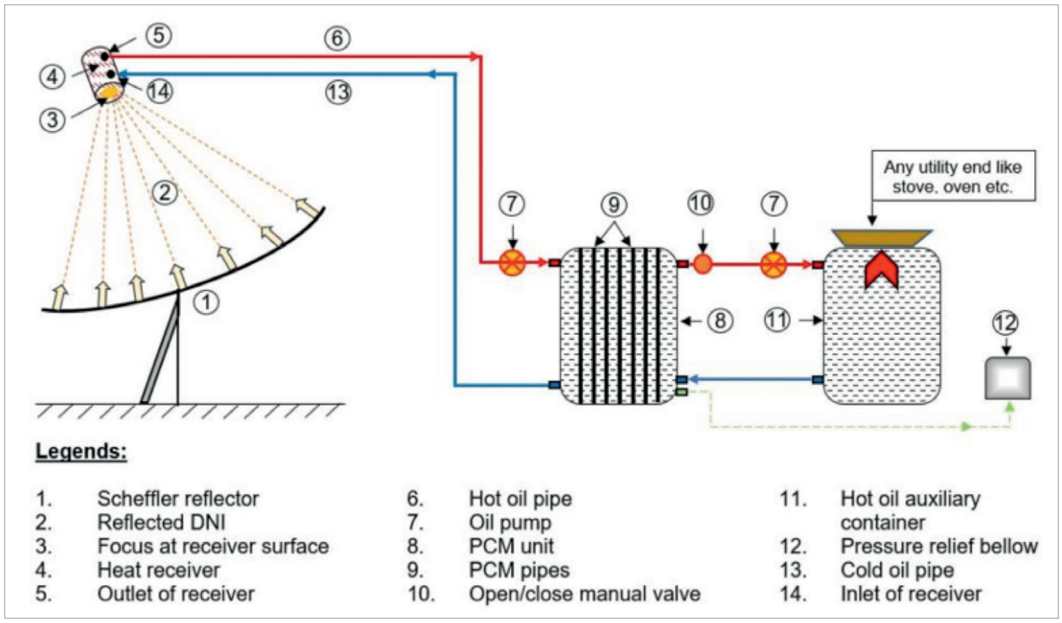

The incoming direct normal irradiance (DNI) strikes at the surface of the Scheffler reflector and converged towards the targeted focus, i.e., surface of the solar heat receiver to produce a temperature greater than 250°C. By circulation of heat transfer fluid (HTF) with a solar powered pump (Heizungs-Umwälzpumpen, EVENES Typ HE-HL+, Light) in the system, heat energy produced at the receiver surface is taken by HTF and conducted to the PCM unit where it is stored. An expansion bellow is also connected in the oil circuit

to release the extra pressure generated in the system which is closed to atmosphere and prevent it from any damage. After discharging the heat energy, HTF is circulated back to the heat receiver to again absorb and convey heat energy from the heat receiver to the system. In this way, the solar PCM system operates continuously to generate the useful heat from solar thermal energy throughout the day. Thermocouple (12), pyranometer and many types of sensors with a digital data logger are also installed in the system at different points to record the real-time data which is being monitored through Control and Monitoring Interface (CMI) online portal.

3.1 Description of Scheffler Reflector for Phase Change Material (PCM) Heat Storage System

Scheffler reflector is used to concentrate and focus the incoming DNI on the heat receiver to produce heat energy as shown in Fig. 3.2. The fabrication of Scheffler reflector was carried out in the Agricultural Engineering workshop, University of Kassel, Witzenhausen, Germany, for the development of the solar PCM system prototype. The main components of the Scheffler reflector are an elliptical reflector frame, a rotating support, tracking channel, reflector stand, and daily and seasonal tracking devices. The I Scheffler reflector was laid by taking the lateral part of a specific paraboloid, and the semi-major and semi-minor axis of an elliptical frame of Scheffler reflector were taken as 210cm and 150cm, respectively. The crossbars were distributed along the minor axis in such a way that one crossbar was installed exactly at the centre of the elliptical frame and the other ones were at equal distance from the preceding one on both sides from the central cross-bar to make the desired section of the paraboloid. The elliptical surface of the Scheffler reflector was made by fixing highly reflective aluminum sheets on the crossbars. The rotating support was fabricated with a steel pipe and equipped with a photovoltaic powered GPS-assisted tracking device to rotate the primary reflector for daily tracking. Daily tracking device rotates the reflector along an axis parallel to the polar axis of the earth with an angular velocity of one revolution per day to counter balance the effect of earth rotation. The reflector stand was placed horizontally on the site in laying position facing towards the sun to utilize maximum DNI during summer.

Figure 3.2: Laying Scheffler reflector (2.5 m²) with GPS assisted daily tracking system.

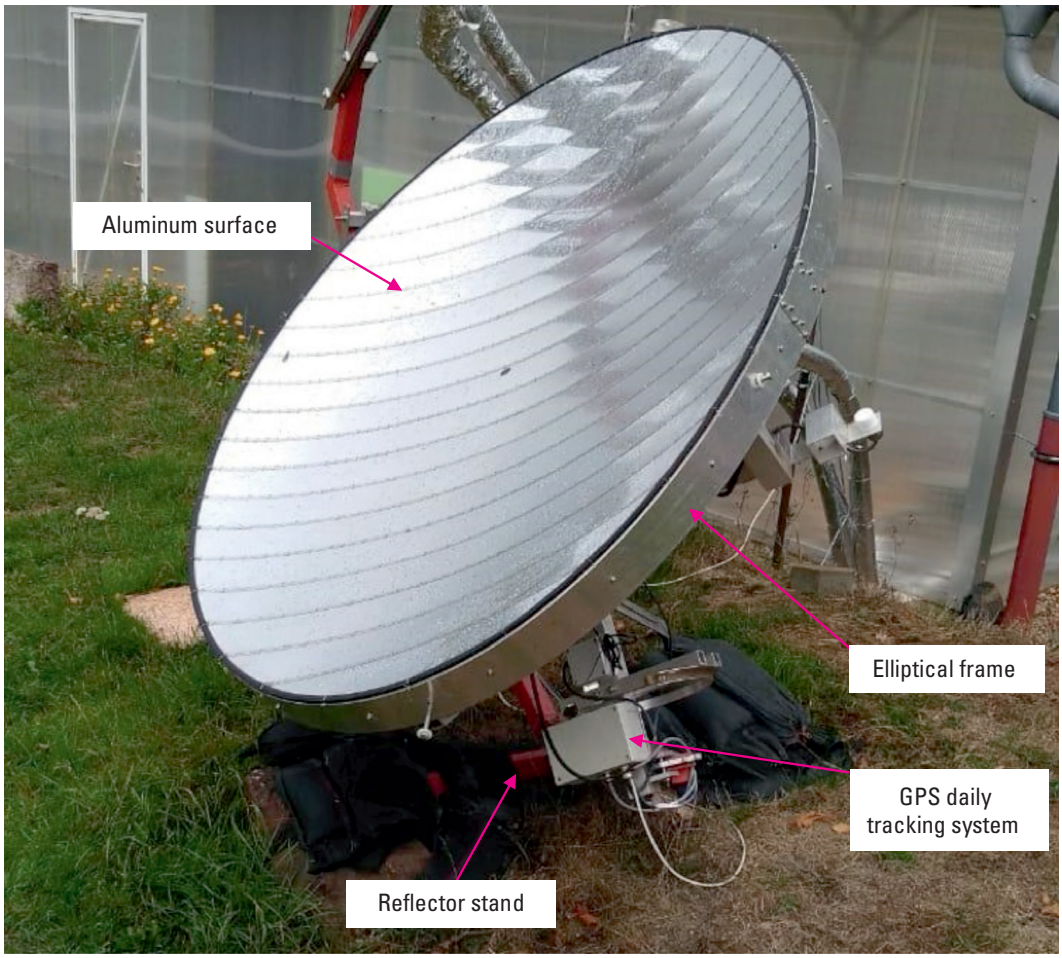

3.2 Heat Receiver

A 220 mm diameter heat receiver comprises a cast aluminum plate surface mounted on the stand of the Scheffler reflector in such a way that the Scheffler reflector targets the incoming DNI exactly at the surface of the heat receiver. Outlet and inlet valves are provided in the heat receiver and attached with 40 mm diameter insulated steel pipes for the flow of HTF (Fragoltherm-32 thermo-oil). All the receiver parts are fixed in a stainless steel (SS) casing which is insulated with 50 mm thick rock wool insulation and wrapped with aluminum foil to prevent heat losses from the receiver. The heat generated at the receiver surface is absorbed and conducted to the PCM heat storage by the flow of HTF inside the receiver. The heat receiver (without insulation) fixed at the laying Scheffler reflector is shown in Fig. 3.3 and complete properties of HTF are given in Appendix-a.

Figure 3.3: Heat receiver mounted on 2.5 m² laying Scheffler reflector (without insulation)

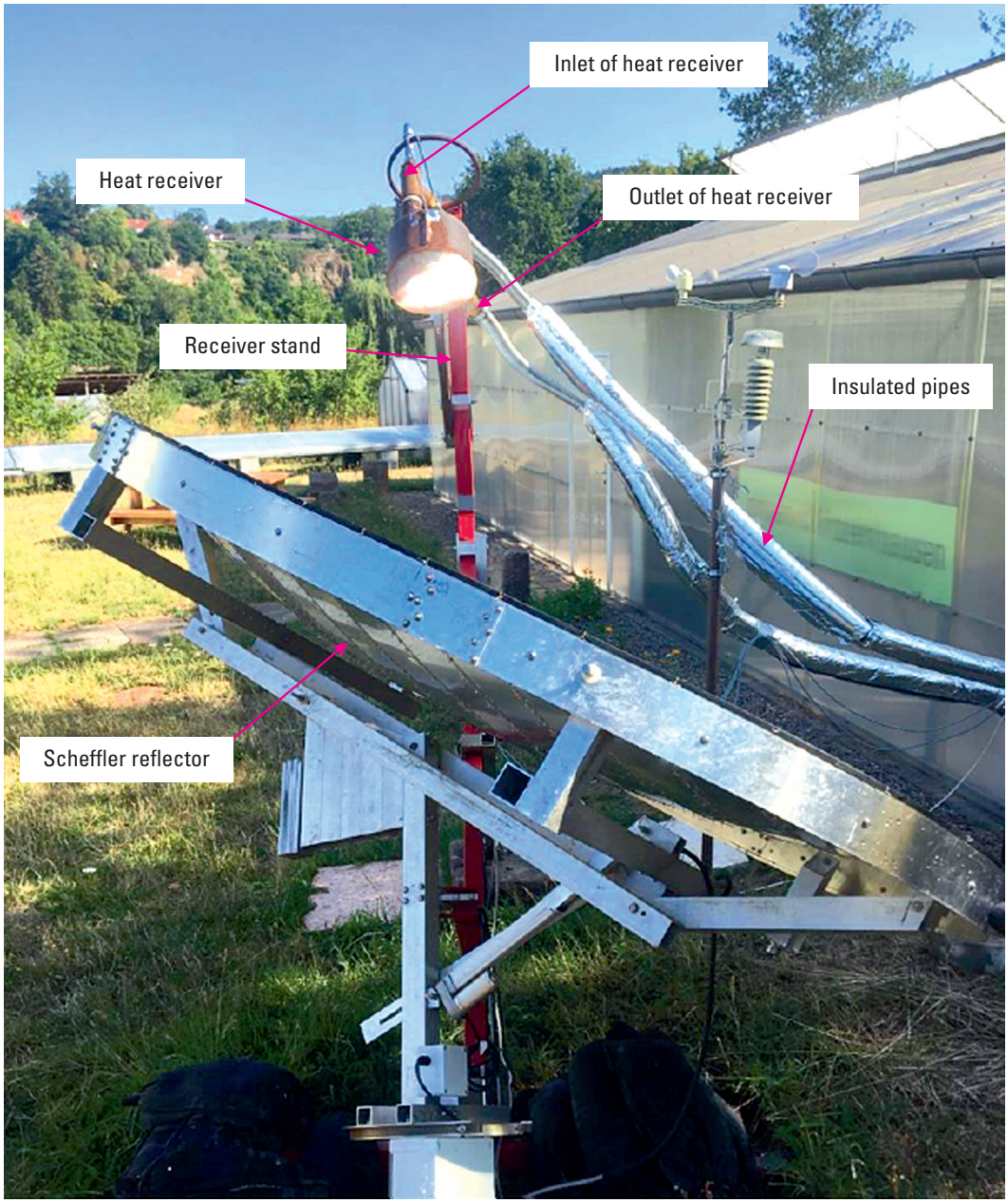

3.3 PCM Heat Storage Unit

The PCM heat storage unit consists of 38 number of tubes of silver steel rings having 30 mm diameter and 870 mm length. The tubes are filled with Mannitol (Roquette) and fixed vertically in a circular iron plate inside a closed cylindrical MS container which is insulated with 50 mm thick layer of rockwool and wrapped by another 50 mm thick insulation layer. HTF absorbs the heat energy from the heat receiver and flows through a 5.3 m long insulated pipe into the PCM unit. Inside the PCM unit, HTF flows around the PCM tubes and transfer the excessive heat energy to PCM through conduction which is utilized later during off sunshine hours. The installation pattern of PCM tubes and insulated PCM unit are shown in Figs 3.4 and 3.5, respectively, and technical specifications of PCM are given in Appendix-B.

Figure 3.4: Installation pattern of PCM tubes

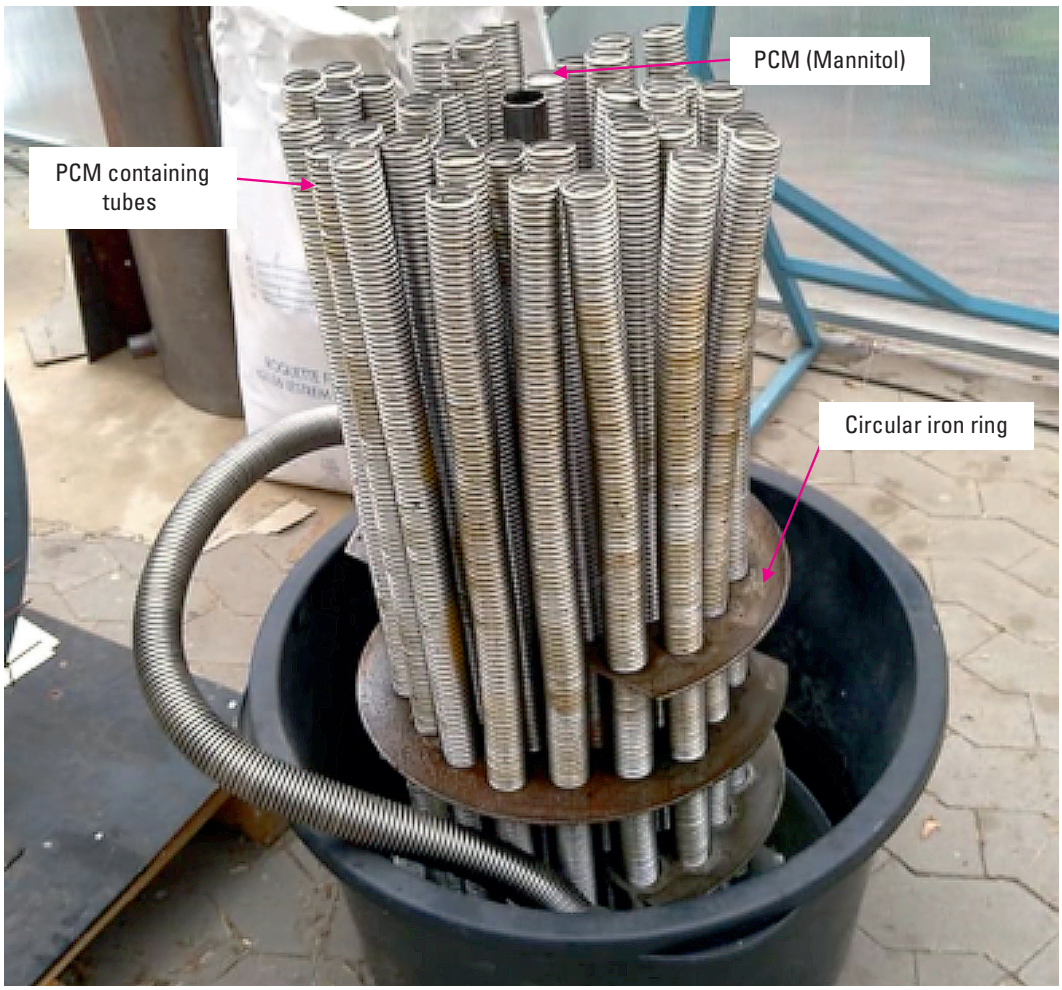

Figure 3.5: Insulated PCM unit

3.4 Expansion Bellow and Accessories

Stainless Steel Expansion Joint, also known as metal bellows, bellows expansion joint, is the compensating element for thermal expansion and relative movement in pipelines, containers, and machines. They consist of one or more metal bellows, connectors at both ends, and tie rods that depend on the application. They are differentiated according to the three basic types of movement—axial, angular, and lateral expansion joints. Stainless Steel Expansion Joint is an elastic vessel that can be compressed when pressure is applied to the outside of the vessel or extended under vacuum. When the pressure or vacuum is released, the bellows will return to its original shape (provided the material has not been stressed past its yield strength). In addition to expansion bellow, there are mountings, fittings, valves, controllers which are directly connected to the system for operation and data acquisition.

Figure 3.6: Pressure relief bellow

3.5 Hot Oil Container

The hot oil container is installed to use stored energy in the PCM and the flow of HTF towards hot oil container is controlled with the help of a valve. Hot HTF flows into the hot oil container where it conducts the stored energy to utility end. After that, HTF flows back from the hot oil container to PCM unit. In this way, the continuous circulation of HTF is carried out for transfer of useful energy throughout the day. Presently, the hot oil container is installed for experimental purposes because this finally available heat energy can be utilized in various decentralized applications.

Figure 3.7: Insulated hot oil container

4 Results and Discussion

The solar PCM system was developed to enhance the solar thermal energy utilization using PCM heat storage for decentralized applications in tropical countries. The design of the system is simple and flexible to produce maximum amount of energy for different post-harvest and food-processing applications at farm level. The performance of the system was evaluated for the estimation of available energy after sunshine hours. Computational fluid dynamic (CFD) analysis was performed to analyze temperature distribution in the PCM and the total available energy with system losses were also determined to optimize the system.

4.1 CFD Analysis of PCM Unit

CFD software was used to simulate temperature distribution using ANSYS workbench which provides a comprehensive suite for modeling fluid flow and other related physical phenomena. In order to avoid the geometry complexity, the targeted part (PCM container) of the system was designed and simulated. Figure 4.1 shows complete layout of the system along with simulated outcomes in the form of temperature profiles of the oil container with PCM pipe. For boundary conditions, pipe containing hot oil towards PCM unit was taken as inlet which received heated oil coming from heat receiver. Data acquired through CMI portal was used to define the boundary conditions. From the temperature profile within the container (fluid and PCM pipes), 45% to 50% of input oil temperature was absorbed in the PCM pipes. In order to visualize temperature distribution in PCM pipes more effectively, the maximum temperature scale was decreased to 49°C. The temperature change of PCM pipes is almost uniform. As hot oil entered into the container and flowed around the PCM pipes, the heat was transferred. This process continued until the oil in the container reached at uniform temperature (up to 95 C). At earlier stage, rate of heat transfer at the top of container could be estimated more (due to large temperature difference between oil and PCM) than at the down side as can be observed from the temperature contours around the PCM pipes. The velocity contour within the PCM unit is also shown in Fig. 4.2.

Figure 4.1: CFD analysis of PCM unit

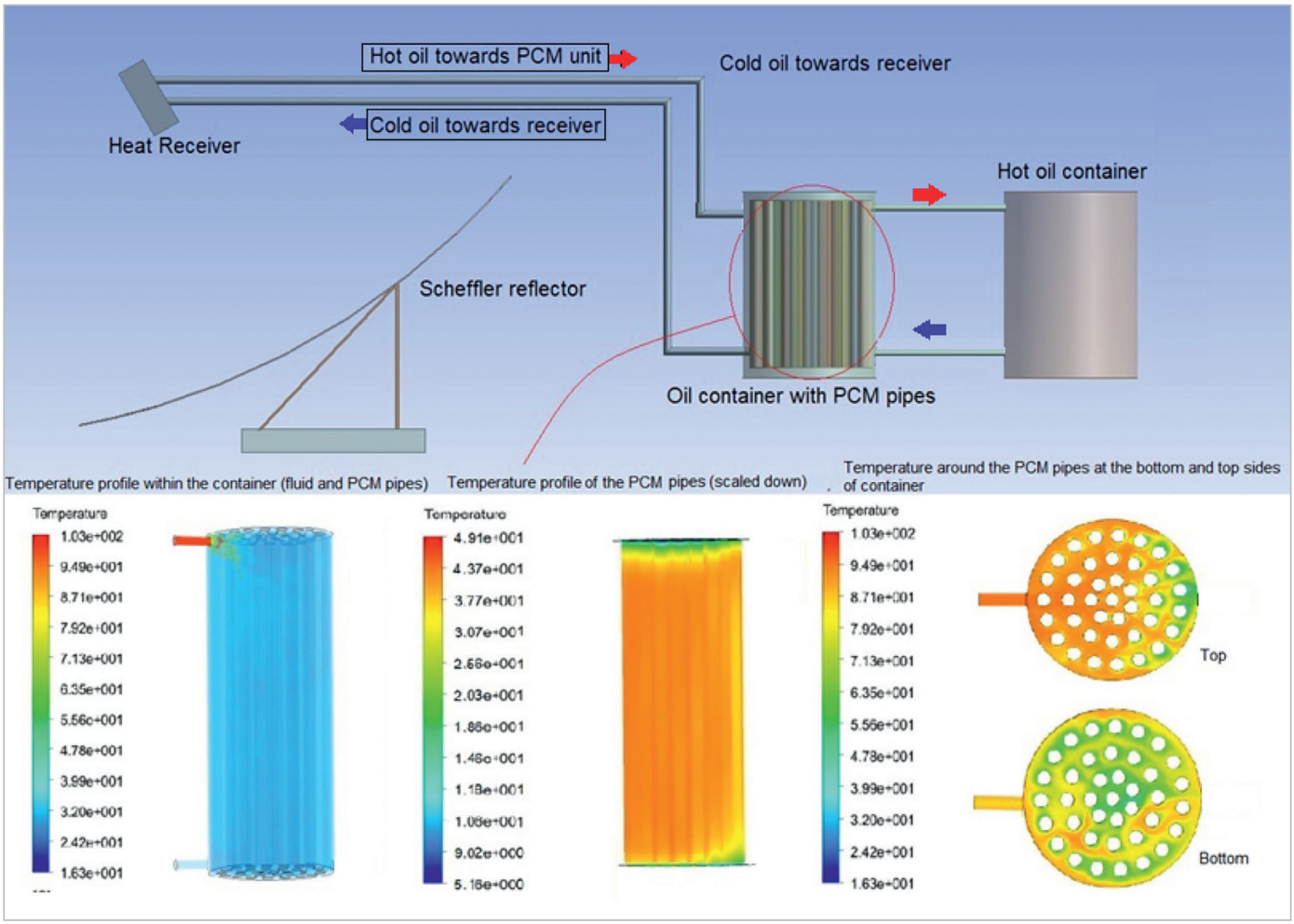

Figure 4.2: Velocity profile of HTF inside the PCM unit

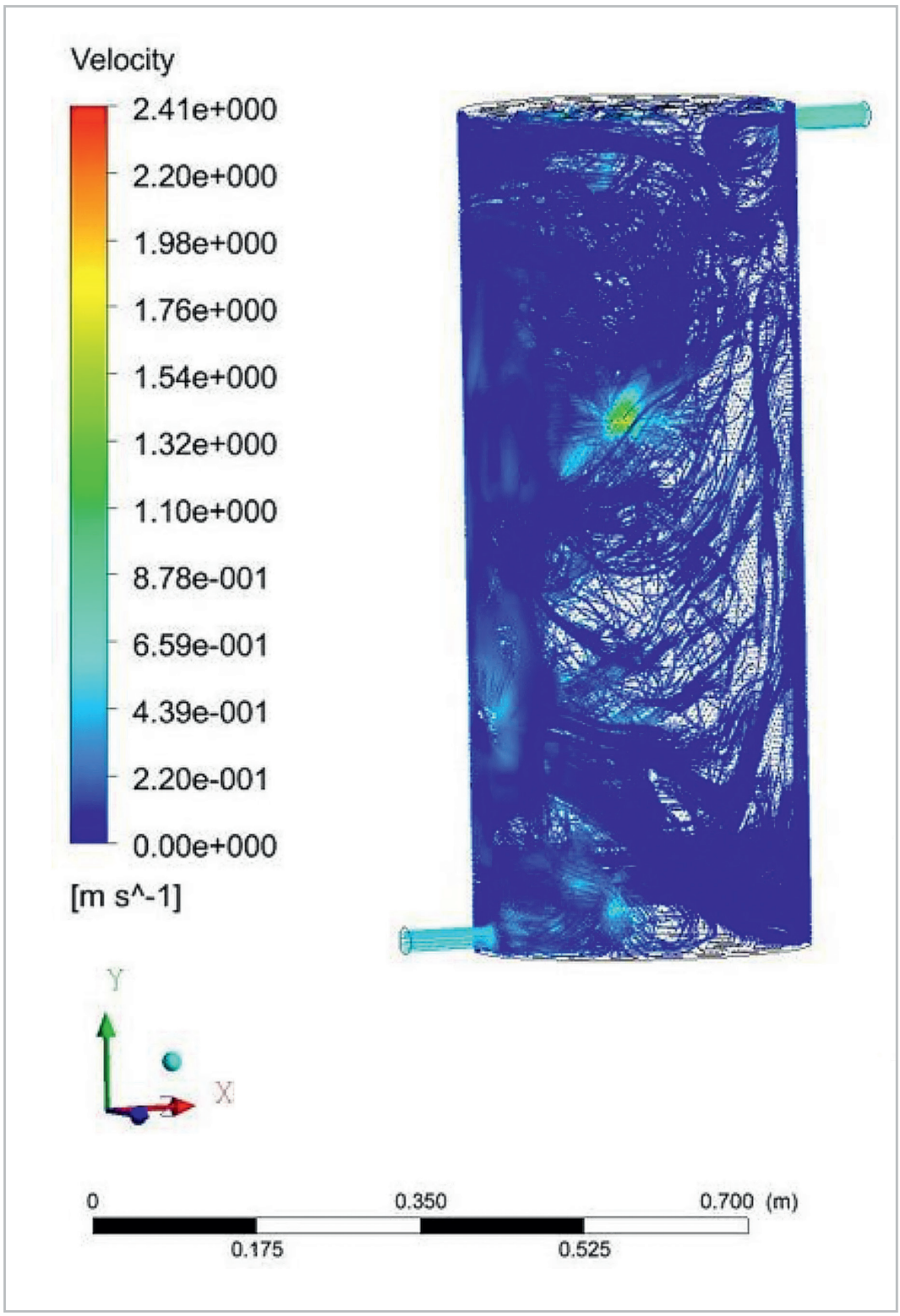

4.2 Energy Analysis of the Solar PCM System

The solar PCM system was also optimized by taking into account different sources of energy losses. The available energy and losses in different components of the entire system are evaluated at five main points including the Scheffler reflector, heat receiver, PCM storage unit, hot oil container, and piping system as represented in Fig. 4.3. The energy analysis is described comprehensively in the following sub-sections.

Figure 4.3: Available energy and losses in different components of solar PCM system

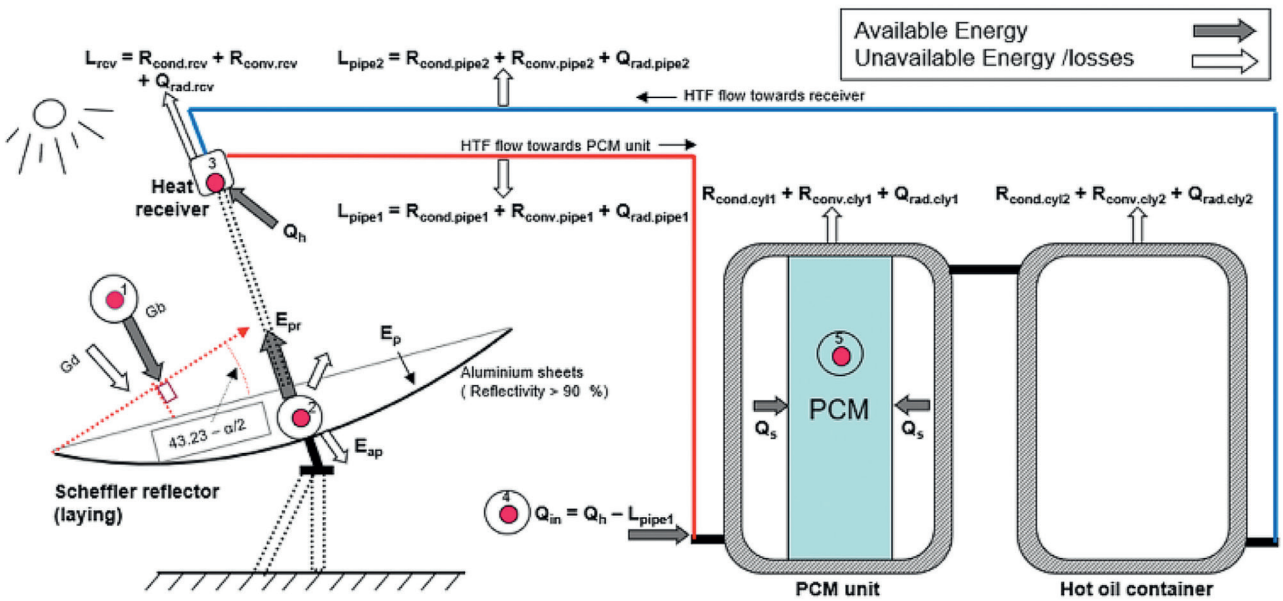

4.2.1 Available Power from the Scheffler Reflector and Its Distribution

The incoming solar radiations are the sum of diffused radiations (G_d) and useful DNI (G_b) among which only the DNI are of useful energy that are falling of the elliptical surface of the Scheffler reflector. The surface of the Scheffler reflector is inclined at an angle of (43.23+α/2) to the falling DNI due to the lateral part of a paraboloid where the solar declination angle (α) is being positive (+) for northern hemisphere and negative (–) for southern hemisphere. Therefore, the aperture area of the Scheffler reflector (Af) is dependent on solar declination angle and is taken as Af× cos (43.23 ± α/2). For the acquisition of DNI data, a pyranometer is installed on the surface of Scheffler reflector in such a manner that it faces directly towards the sun for measuring the intensity of the incoming DNI the whole day. In this way, the total input energy available (Ep) at the surface of the Scheffler reflector is the DNI recorded by pyranometer times this fraction of the area Af*cos (43.23 ± α/2) and is given in the mathematical form.

$$E_p = G_b A_f cos\,(43.23 \pm \frac{\alpha}{2}) \tag{4.1}$$

also

$$A_s = A_f cos\,(43.23 \pm \frac{\alpha}{2}) \tag{4.2}$$

where As is the available aperture area of the Scheffler reflector at any day of the year.

As the Scheffler reflector is elliptical, the surface area can also be expressed in terms of semi-minor axis and semi-major axis. Eq. (4.2) can also be expressed as:

$$A_s = (\pi ab - 0.1) \times cos\,(43.23 \pm \frac{\alpha}{2}) \tag{4.3}$$

where a and b are the semi-minor axis and semi-major axis of the elliptical frame of the Scheffler reflector and α is the solar declination.

The solar declination angle (α) is calculated by the equation given by Duffie and Beckman (2006) with the least error (Error < 0.035°).

$$\begin{aligned}\alpha = (180/\pi)[&0.006918 - 0.399912\ cos(n-1)2\pi/365 + 0.070257\ sin(n-1)]2\pi/365 \\ &- 0.006758\ cos\ 2(n-1)2\pi/365 + 0.000907\ sin\ 2(n-1)2\pi/365 - 0.002679\ cos\ 3(n-1)2\pi/365 \\ &0.00148\ sin\ 3(n-1)2\pi/365\end{aligned} \tag{4.4}$$

where "n" is the day of the year and "α" is solar declination angle.

Solar declination angle (α) varies from –23.5° on Winter solstice (December 21) to +23.5° on Summer solstice(June 21). A simplified view of sun's trajectory on the sky on different Solstices and Equinox is shown in Fig. 4.4.

Figure 4.4: Sun's trajectory at Winter Solstice, Summer Solstice and Equinox

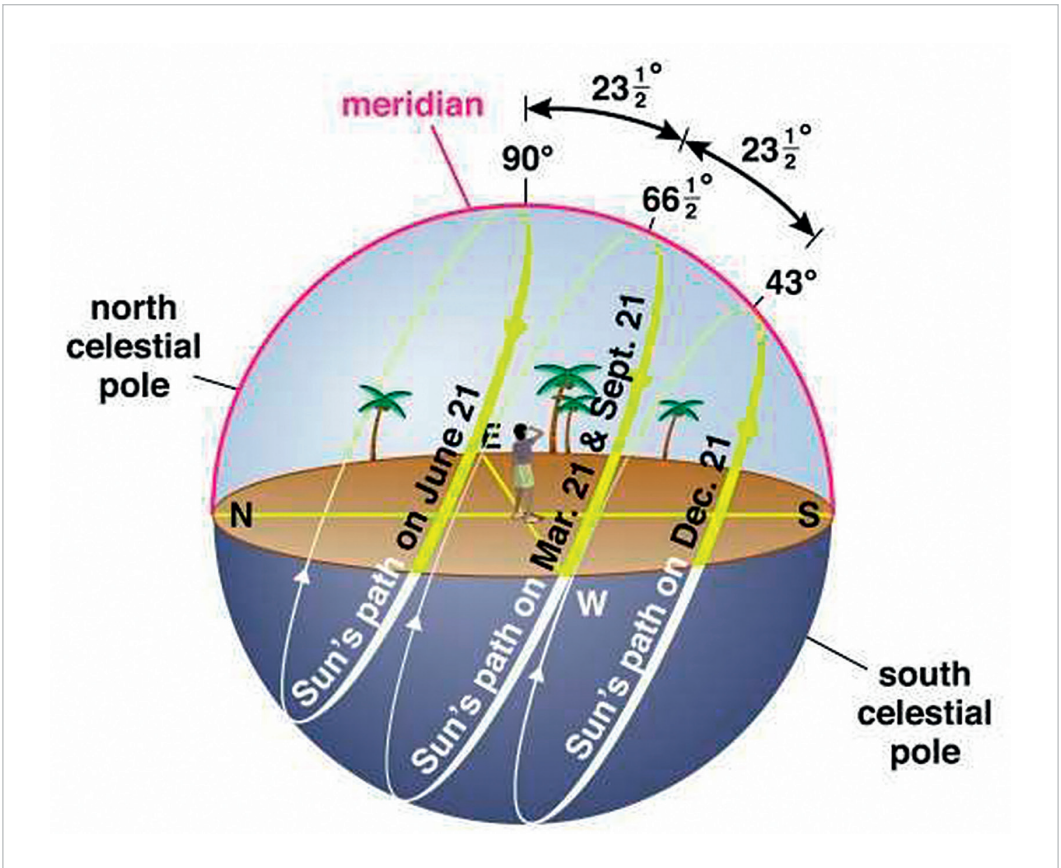

Source: Noosphere, 2012

The variation of solar declination (α) and aperture area for a 2.5 m^2 laying Scheffler reflector in northern hemispheres during the entire year is shown in Fig. 4.5. It is evident from Fig. 4.5 that the aperture area of the laid Scheffler reflector increases with increase in solar declination angle and vice versa, hence showing a direct correlation between them. The aperture area is maximum on winter solstice (1.44 m^2), minimum on summer solstice (2.13 m^2) and found to be similar at equinox (m^2) in the northern hemisphere for the laying reflectors. For a specific size of laying Scheffler reflector, more energy can be obtained with the same DNI in summer season as compared to winter season. The laying Scheffler reflectors are more suitable to get maximum power as they directly focus on the sun light on targeted area and eliminates the necessity of secondary reflector.

Figure 4.5: Variation of solar declination and aperture area of Scheffler reflector in the northern hemisphere (valid for 2.5 m² laying reflectors)

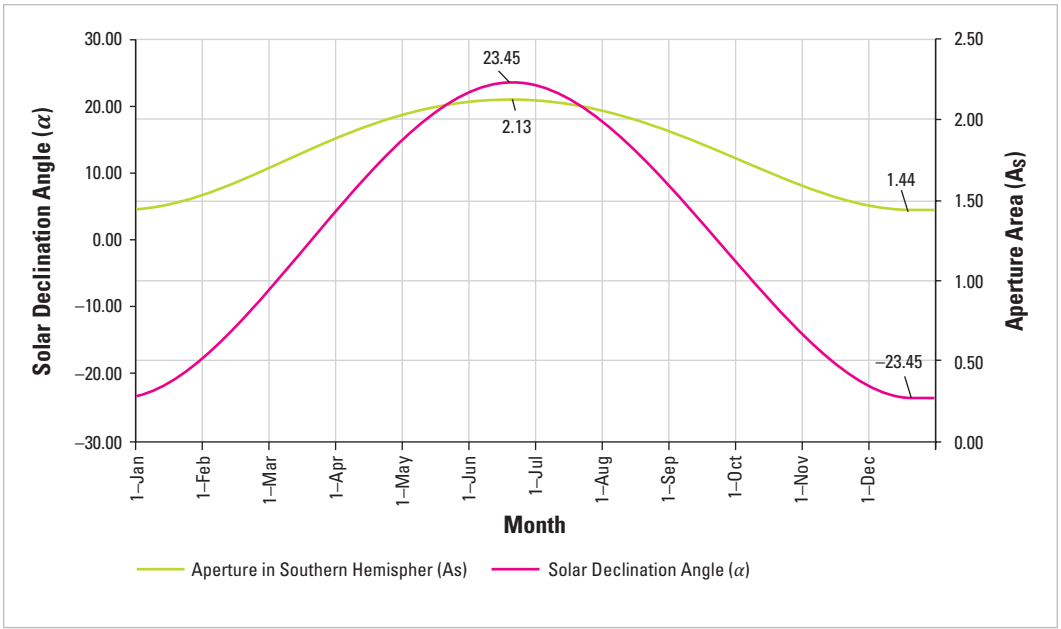

The surface of the Scheffler reflector is made of highly reflective aluminum (specific reflectance >90 %) sheets which converge the incoming useful DNI towards heat receiver. Some part of the incoming radiation is absorbed by the surface of the Scheffler reflector, therefore the available energy after the Scheffler reflector (Epr) is given by:

$$E_{pr} = R_p E_p \tag{4.5}$$

where, Rp is the reflectivity of the surface of the Scheffler reflector.

Generally, out-of-focus radiation is also taken into account from the Scheffler reflector but as the present one is developed in a highly precise manner, the fraction of out-of-focus radiation (Ff) is considered as only 5 %. The remaining radiation is the useful power available at the surface of heat receiver and calculated as:

$$E_s = E_{pr} F_f \tag{4.6}$$

4.2.2 Energy Distribution and Losses at Solar Heat Receiver

Infrared camera was also used during the experiments for capturing the thermal images of solar heat receiver to observe power distribution as well as to measure the fraction of power available from converged DNI at the heat receiver. During the experiment on September 5, 2018 at 01:25 p.m., the position of Scheffler reflector is shown in Fig. 4.6. It was visually observed that the Scheffler reflector perfectly focus the incoming DNI at the surface of the heat receiver for power generation throughout the day as shown in Appendix-D. At the same time thermal images by infrared camera shows a temperature of 153.19 C at the centre of the heat receiver surface as represented in Fig. 4.7. It is clear that the temperature decreases gradually towards the outer edges of the heat receiver surface. This is due to the fact that the Scheffler reflector produces maximum intensity of focused DNI in the middle of the focus area. Overall, a good temperature distribution was observed on the surface of the heat receiver which allows efficient heat transfer to the HTF flowing inside the heat receiver. These results are also consistent with theoretically calculated results which provide the justification for the design configuration of the Scheffler reflector and appropriate heat receiver.

Figure 4.6: Position and targeted focus of 2.5 m^2 laying Scheffler reflector in southern hemisphere on September 5, 2018 at 01:25 p.m. with 781 W/m^2 DNI

Figure 4.7: Infrared thermal image of temperature distribution on heat receiver on September 5, 2018 at 01:25 p.m. with 781 W/m²DNI

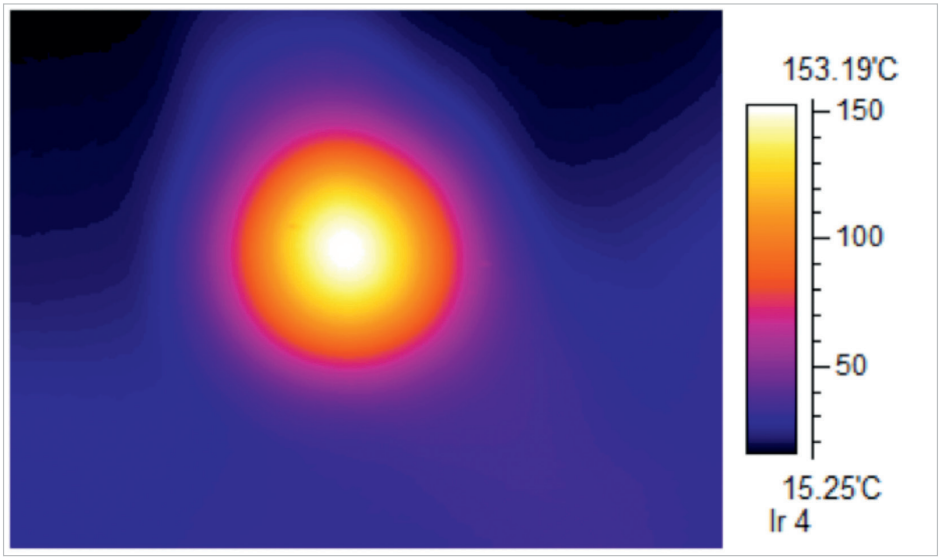

Along with the power generation, heat energy is also lost from the outer side walls, back side and pipe-fittings of the heat receiver as it was not insulated. The outer side wall and back side surface temperature, and the temperature of pipe-fittings of the heat receiver were observed to be 88°C and 52°C, respectively, as shown in Fig. 4.8.

Figure 4.8: Infrared thermal image of temperature distribution on side walls and back side surface, and pipe-fittings of heat receiver of solar PCM system

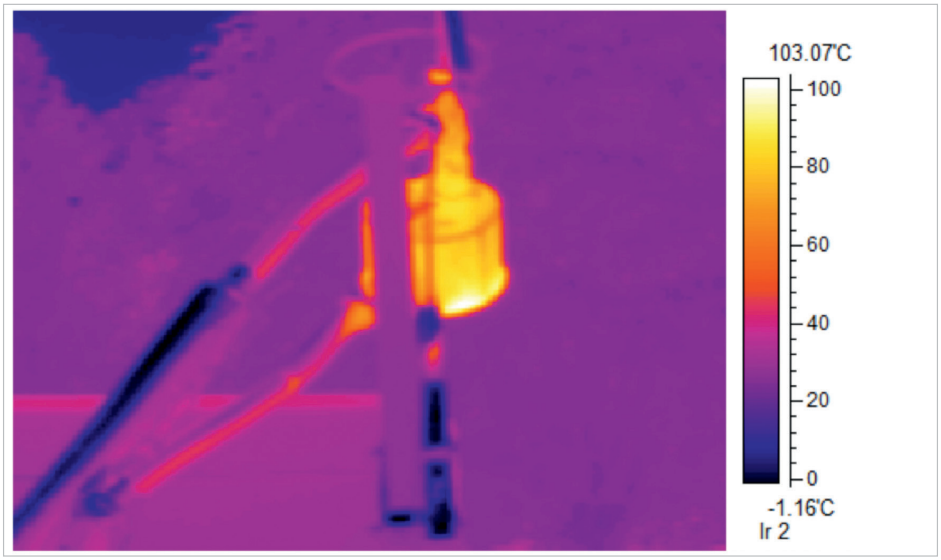

The results have shown that significant heat losses were taking place from the receiver due to improper insulation. This huge heat loss (> 50 %) was reduced by insulating the sides and back of the heat receiver with 50mm-thick layer of rockwool insulation wrapped with 50mm aluminum foil; the reduction in thermal losses were calculated.

4.2.3 Thermal Losses Calculations for the Solar PCM System

The heat absorbed per unit time by HTF flowing inside a receiver was dependent on the specific heat of HTF (Cph), HTF mass flow rate (mf), and entry temperature (Ti) and exit temperature (Tf) of HTF. The energy absorbed by the HTF (Qh) is calculated as under (Duffie and Beckman, 2006):

$$Q_h = m_f C_{ph}(T_o - T_i) \tag{4.7}$$

The steady state heat transfer (φ) through a cylindrical layer that is exposed to convection on both sides to fluids is given as (Cengel, 2006):

$$\varphi = \frac{(T_{in} - T_{amb})}{R_{cond} + R_{conv}} \tag{4.8}$$

where Tin, Tamb, Rcond and Rconv are inside oil temperature, ambient temperature, conduction resistance, and convection resistance, respectively.

Thermal conduction resistance for the cylindrical part is determined using following relation (Cengel, 2006):

$$R_{cond.c} = \frac{1}{2\pi\lambda L}\ln\left(\frac{r_{ext}}{r_{int}}\right) \tag{4.9}$$

where λ, L, rext, and rint are the thermal conductivity of the material used, lateral length of the cylindrical surface, external and internal radius of the cylinder, respectively.

The conduction resistance for a plane surface is determined using the following relation (Cengel, 2006):

$$R_{cond.p} = \frac{t}{\lambda A} \tag{4.10}$$

where t and R are the thickness and cross-sectional area of surface, respectively.

With insulation, the conductive resistance for the multilayered cylindrical and plane walls is determined by adding the conductive resistance for all layers and is generalized as:

$$R_{cond} = \sum R_{cond}^{i} \tag{4.11}$$

where "i" indicates any layer of any material with their respective thermal conductivity and thickness.

Convection resistance is determined using the following relation:

$$R_{conv} = \frac{1}{hS} \tag{4.12}$$

where h is the natural convection coefficient and S is the external surface area.

Radiation heat losses are determined using the following relation:

$$Radiation\ losses = \varepsilon\ \sigma\ S\ (T_{ext}^{4} - T_{space}^{4}) \tag{4.13}$$

where ε is the emissivity, σ is the Stephen Boltzmann constant, Tspace is the space temperature (K), Text is the external surface temperature (K) and is determined by the following formula:

$$T_{ext} = T_{amb} + \varphi R_{conv} \tag{4.14}$$

By substituting the value of T_{ext} in Eq. 3.24, the total radiation heat losses are determined. By adding all the losses, the total losses of the system can be calculated.

4.2.4 Determination of natural convection coefficient

The value of "h" depends on the properties of the fluid (air), geometry and position of the component. In order to calculate the actual values of natural convectional coefficients, the following equations are used (Jannot, 2003).

$$h_1 = \frac{Nu_1 \lambda_a}{L} \tag{4.16}$$

$$h_2 = \frac{Nu_2 \lambda_a}{L} \tag{4.17}$$

where

$$Nu_1 = 0.59 PrGr^{0.25} \tag{4.18}$$

$$Nu_2 = 0.021 PrGr^{2/5} \tag{4.19}$$

where Prandtl No. (Pr) is given as under:

$$Pr = \frac{C_a u_a}{\lambda_a} \tag{4.20}$$

where Cais the air heat capacity (1009 J kg^{-1} K^{-1}), μa is the dynamical viscosity of air (0.000020500 Pa s), λaIS the thermal conductivity of air (0.0295 W m^{-1} K^{-1}).

By substituting this value in Eq. 3.29, we get Pr = 0.7011694915

This value of Pr will remain constant as it comprises of only parameters regarding atmospheric air.

Also,

$$G_r = \frac{2g(T_{ext} - T_{amb})\rho^3 L^3}{u^2(T_{ext} + T_{amb} + 273.5)} \tag{4.21}$$

where Tamb is the air ambient temperature (20 ℃), ρ is the density of air (1.050 Kg/m^3). By substituting the values of ρ, μ, T_{ext} and T_{amb} in Eq. 3.30, the value of Gr is calculated. Thereafter, the value of the product "GrPr" is calculated.

The heat storage potential of the phase change materials (PCM) is important and the energy storage for a range of temperature including the melting point is:

$$Q_s = \int_{T_1}^{T_m} mC_p dT + mh + \int_{T_m}^{T_2} mC_p dT \tag{4.22}$$

Where Qs is the total amount of energy stored (J), mis the mass of the medium (kg), Cpis the specific heat of the medium (solid below Tm, liquid over), potentially temperature dependent (J/kg.K), his the latent heat (J/kg), Tm is the melting temperature, and T1 and T2 are the initial and final temperatures of the relevant range (K), respectively (Mussard, 2013).

4.3 Output of Mathematical Modeling

An algorithm has been developed using design configuration and available parameters of the solar PCM system. For a case study, the predicted output on a sunny day of September 5, 2018 with DNI of 781 W/m^2 using mathematical model for the thermal losses in solar PCM system is shown in Fig. 4.9.

Figure 4.9: Predicted values of thermal losses per unit time from solar PCM system (for the laying reflectors in the northern hemisphere for 781 W/m^2 on September 5, 2018)

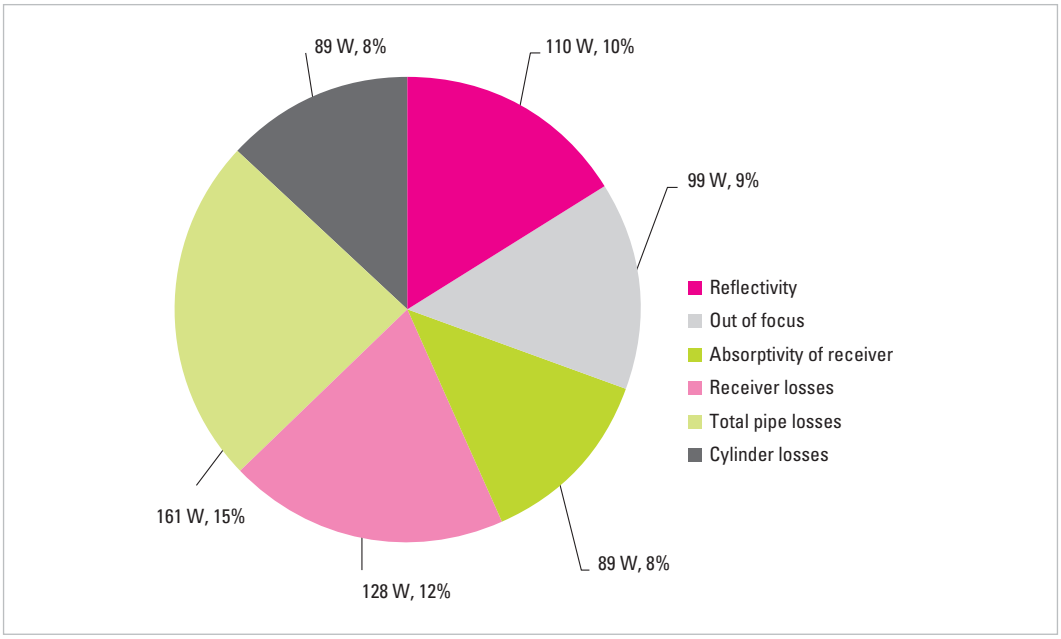

Fig. 4.9 shows the heat energy losses from the solar PCM system. In the present input data set, solar PCM system was run in solar and irrigation campus, Witzenhausen, Germany on September 5, 2018 with DNI of 781 W/m^2 under similar conditions. The heat energy losses per unit time (W) due to the lack of reflectivity from the Scheffler reflector, out of focus radiations at the targeted area, absorptivity of heat receiver, piping system losses, and cylinder losses (in the form of conduction, convection and radiations using 50 mm insulation thickness) were found to be 110W, 99W, 89W, 128W, 161W, and 89W, respectively. Their corresponding percentage losses are found to be 10 %, 9 %, 8 %, 12 %, 15 %, and 8 %, respectively. The final available energy in the PCM was found to be 414 W (38 %). In terms of components of solar PCM system, the heat losses from the Scheffler reflector, heat receiver, and the entire piping system were found to be 209W, 217W, and 161W with their percentage 19 %, 20 %, and 15 %, respectively. Available energy per unit time at different components during the performance evaluation on September 5, 2018 is shown in Fig. 4.10.

Figure 4.10: Power distribution sequence and available power in the solar PCM system (predicted results for solar and irrigation demonstration plant, Witzenhausen on September 5, 2018)

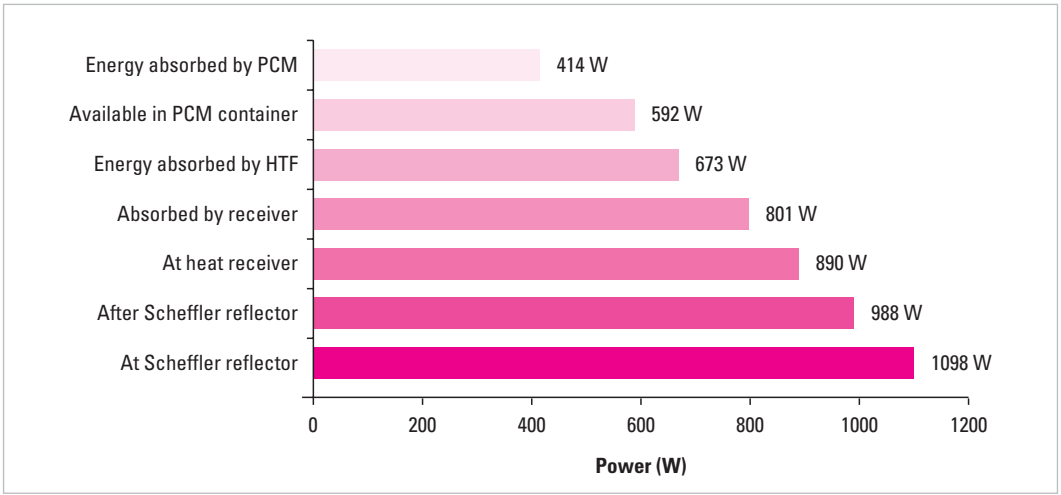

It can be seen from Fig. 4.10 that the total available energy on Scheffler reflector was 1098W and after all losses, final available energy to PCM was 414W. The efficiency of the system was found to be 37.76%. These results of mathematical modeling were found similar to the experimental results under the same conditions. Therefore, the model can be applied in the northern hemisphere under the existing condition of the system. However, the DNI will vary according to latitude of the location.

4.4 Energy available for PCM

The graphical presentation of total DNI power, power available at the Scheffler reflector and final available power for the PCM against 800 W/m^2 for summer solstice, equinox, and winter solstice (for the laying reflectors in the northern hemisphere) is given in Fig. 4.10. From the mathematical model, power available at the 2.5 m^2 Scheffler reflector for summer solstice, equinox, and winter solstice were found to be 1310W, 1124W, and 882W, respectively at 800 W/m^2 DNI for laying reflectors in the northern hemisphere. With the same intensity of DNI, the power absorbed by PCM in summer solstice, equinox, and winter solstice were found to be 494W, 424W, and 333W, respectively, which can be utilized after sunshine hour for prolonging the availability of heat. These modeling results of solar PCM system provide useful information to predict the total power available on the reflector and available energy for PCM against a wide range of DNI.

Figure 4.11: Available power distribution for solar PCM system with 800 W/m^2 for summer solstice, equinox, and winter solstice (for 2.5 m^2 laying Scheffler reflector in northern hemisphere)

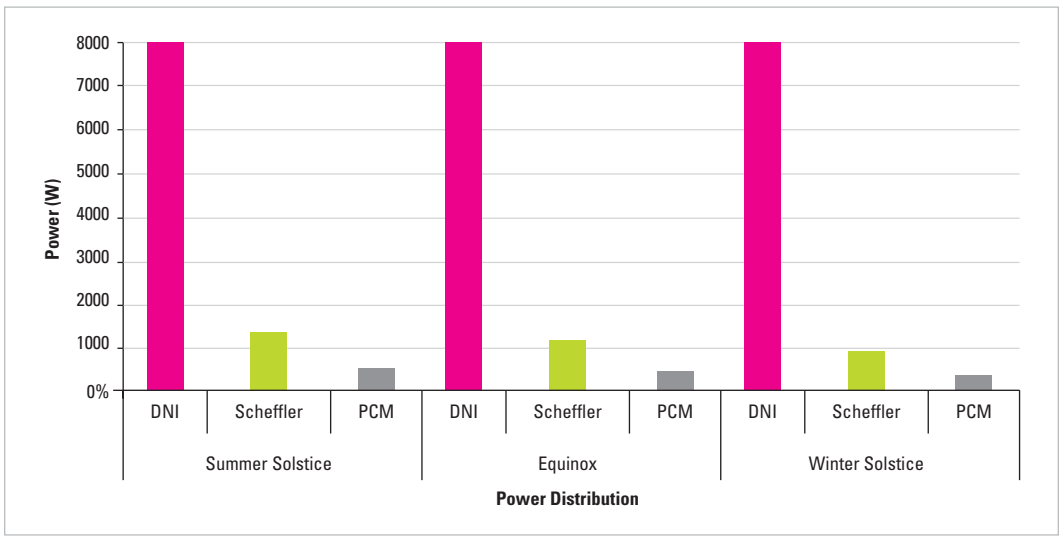

4.5 Results of the Experimental Set-up

Data were recorded for Buffer Tank 1 and Buffer Tank 2 at various points (upper and lower side as well as at inner and outer sides of the thermal oil and PCM)) with the help of a data-logger and this real-time data is available online. The temperature variation at different points in the solar PCM system for September 5, 2018 is recorded through online CMI portal and represented graphically in Fig. 4.11 whereas the complete logged data from June to October 2018 are given in Appendix-C.

It has been observed that a maximum temperature recorded was up to 110°C temperature at the receiver and approximately, the same temperature was available at the inlet side of Buffer Tank No. 1. However, there was a slight decline of the temperature from the bottom side of Buffer Tank 1. At day time, Buffer Tank No. 2 was not taken in circuit and its pump was not made operational and these lines are just showing the room temperature.

Figure 4.12: CMI portal graph for temperature variation at different point in the solar PCM system at solar and irrigation demonstration plant, Witzenhausen on September 5, 2018

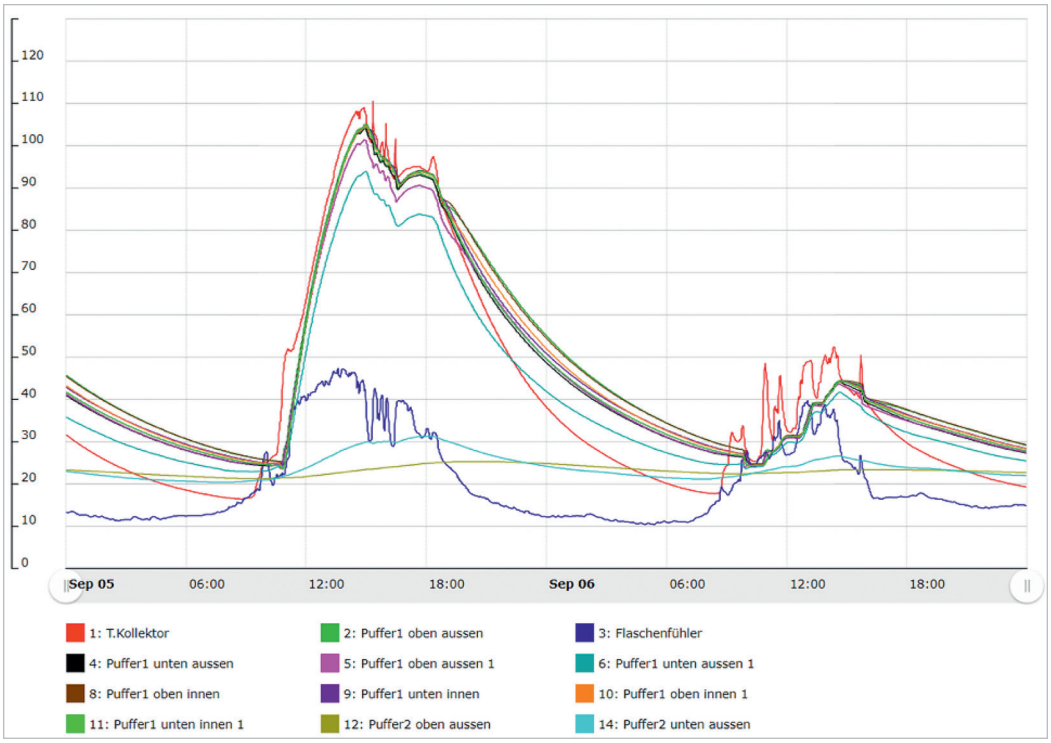

4.6 Overall Discussion

Fabrication and performance evaluation results of a novel solar PCM system have been presented in the current research work. A comprehensive literature was reviewed regarding design configurations, PCM selection, utilization, and scope of PCM in decentralized agricultural processing before the development stage. The solar PCM system was entirely developed at the solar and irrigation demonstration plant, Witzenhausen (51°20′32″N 9°51′28″E) by the collaboration of three institutes and mainly comprises a 2.5 m^2 laying Scheffler reflector, piping system, PCM unit, and a hot oil auxiliary container. The specific aim of this innovative technology is to overcome the necessity of fossil-fuels-based energy supplies during the cloudy weather or after sunshine hours by providing continuous supply of solar energy with thermal energy storage for the on-farm solar food processing applications.

A mathematical model was developed to test the design configurations of the solar PCM system and predict the output energy distribution for a given data set. For a sample input of data (September 5, 2018), output of mathematical model showed 414 W energy was available to the PCM from the total available power of 1098 W with 781 W/m^2 of DNI. Heat losses from the Scheffler reflector, heat receiver, and entire piping system were found to be 209W, 217W, and 161W with their percentage 19%, 20%, and 15%, respectively. The overall system efficiency was found to be 38%.

The laying Scheffler reflector attached with a GPS sun-tracking system provided a precise focus of concentrated DNI at the heat receiver and a maximum temperature of 153.19°C was recorded on the surface of the heat receiver during the trials. Various thermocouples and temperature sensors were installed at different components to observe the temperature variations and energy losses in the system. All the field trials data were recorded with a digital data logger and stored in a specially designed online CMI portal for further calculations. The predicted results of mathematical model and real-time observations were found to be consistent and showed satisfactory heat distribution according to the design configurations of the solar PCM system. CFD analysis of PCM unit were also performed which showed almost uniform heat transfer and temperature distribution inside the PCM unit. Inside the PCM unit, about 87°C–95°C temperature of hot thermal oil was achievable that allowed to transfer approximately 50% of heat energy to the PCM by raising its temperature up to 48°C under the equilibrium state of the system. This stored energy can be utilized at the times when the input energy from DNI becomes lower. An auxiliary hot oil container was attached to the PCM unit for the utilization of stored energy in any subsequent process.

Although the solar PCM system is a state-of-the-art step towards solar thermal heat storage technologies using PCM, some design flaws are also present in the system. For example, the maximum temperature obtained inside the heat receiver during the whole experimentation period was 110°C on September 5, 2018 which is far much lower than the melting temperature (~167°C) of PCM used (Mannitol) and 8% of this already inadequate energy is further lost before entering in the PCM unit due to lengthy pipe lines. The technical solutions in a comprehensive manner for all the possible deficiencies of the system are given in the recommendations section.

5 Conclusions

the solar PCM system was indigenously designed to enhance solar thermal energy utilization after sunshine hours for decentralized applications in agricultural processing. With the present design configurations of the system, CFD simulations showed a good uniform temperature distribution inside the PCM unit and it was also observed that 45%–50% of the heat was transferred by the HTF to PCM. Although PCM showed good response for heat absorption, it did not change its phase from solid to liquid during the trials due to insufficient input energy. Therefore, it was concluded that the size of the Scheffler reflector needs to be bigger for greater energy input. Mathematical modeling results showed 209W (19%), 217W (20%), and 161W (15%) heat losses from the Scheffler reflector, heat receiver, and entire piping system, respectively with an overall system efficiency of 38%. In terms of parts, the heat energy losses per unit time (W) due to the lack of reflectivity from the Scheffler reflector, out of focus radiations at the targeted area, absorptivity of heat receiver, piping system losses, and cylinder losses (in the form of conduction, convection and radiations using 50 mm insulation thickness) were found to be 110W (10%), 99W (9%), 89W (8%), 128W (12%), 161W (15%), and 89W (8%), respectively. Overall, the solar PCM system provides an excellent technical platform to address the solar thermal energy storage issues.

Recommendations

- It is recommended to employ a larger size of Scheffler reflector to produce more thermal power from the available DNI for the existing system to change the phase of the PCM used and utilize high value of latent heat in addition to sensible heat for all-time operation of the system.
- It is recommended to improve the design of the heat receiver in such a way that the PCM can be directly used inside the receiver for effective heat transfer, so that the phase of the material can efficiently be changed, i.e., solid to liquid.
- It is recommended to use copper material in the receiver instead of casted aluminum as copper has almost double thermal conductivity than the aluminum.
- Use of a high-quality glass cover to cover the receiver surface is also recommended to minimize heat losses from the receiver.
- The length of the piping system should be reduced to decrease the heat conveyance losses in pipes (15%) which will increase the available energy for PCM in the existing design.
- The system should also be evaluated by using other PCM material-like Eutectic mixture of KNO3/NaNO3.
- Trials should be conducted at different flow rates of thermal oil to investigate the optimum parameters of heat transfer rate.

Acknowledgements

The author highly acknowledges “International Centre for Development and Decent Work (ICDD)” and “German Academic Exchange Service (DAAD)”, Germany for the financial support and providing opportunity to conduct this research work under the Ela Bhatt Professorship from June 1 to September 30, 2018. The author also thanks Prof. Dr. Oliver Hensel and Dr. Christian Dede, Department of Agricultural and Biosystems Engineering (AGT), Witzenhausen, for providing facilities and technical help/guidance in conducting this research work.

References

- **Abdelaziz, E.A., R. Saidur, and S. Mekhilef. 2011.** A review on energy saving strategies in industrial sector. Renewable and Sustainable Energy Reviews,15(1): 150–68.
- **Acharya, H.N. and A.C. Chandak. 2013.** Production of plaster of paris using solar energy. International Journal of Research in Engineering and Technology, 2(4): 516–19.
- **Afzal, A., A. Munir, A. Ghafoor, and A.A. Alvardo. 2017.** Development of hybrid distillation system for essential oil extraction. Renewable Energy, 113: 22–29.
- **Ahmet K., H.F. Oztopb, T. Koyunc, and Y. Varol. 2008.** Energy and exergy analysis of a latent heat storage system with phase change material for a solar collector. Renewable Energy, 33(4): 567–74.
- **Akhade, A.M. and R.J. Patil. 2015.** Design, fabrication and analysis of Scheffler reflector. International Engineering Research Journal, 2: 2842–44.
- **Akorede, M.F., H. Hizam, M.Z.A. Ab Kadir, I. Aris, and S.D. Buba. 2012.** Mitigating the anthropogenic global warming in the electric power industry. Renewable and Sustainable Energy Reviews, 16(2012): 2747–61.
- **Arce, P., M. Medrano, A. Gil, E. Oró, and L.F. Cabeza. 2011.** Overview of thermal energy storage (TES) potential energy savings and climate change mitigation in Spain and Europe. Applied Energy https://doi.org/10.1016/j.apenergy.2011.01.067
- **Bal, L.M., S. Satya, and S. N. Naik. 2010.** Solar dryer with thermal energy storage systems for drying agricultural food products: a review. Renew Sust. Energ. Rev. 14: 2298–2314.
- **Barker, T., I. Bashmakov, L. Bernstein, J.E. Bogner, P.R. Bosch, and R. Dave. 2007.** Technical summary, in Climate change 2007: mitigation. Contribution of Working Group III to the Fourth Assessment Report of the Intergovernmental Panel on Climate Change. Cambridge, United Kingdom/New York, NY, USA: Cambridge University Press, pp. 1–70.
- **Bennamoun, L. 2013.** Improving solar dryers' performances using design and thermal heat storage. Food Eng. Rev, 5: 230–48.
- **Castell, A., C. Solé, M. Medrano, J. Roca, L. F. Cabeza, and D. García. 2008.** Natural convection heat transfer coefficients in phase change material (PCM) modules with external vertical fins. Applied Thermal Engineering, 28(13): 1676–86.
- **Cengel, A. Y. 2006.** Heat and mass transfer, A practical approach (3rd Ed.). McGraw-Hill Companies, Inc. 1221-Avenue, NY-10020, New York, USA.

- **Chandak, A. and S.K. Somani. 2009.** Design of multistage evaporators for integrating with Scheffler Solar concentrators for food processing applications. In: Proceedings of international solar food processing conference.

- **Chandrashekara, M. and A.J. Yadav. 2017.** Experimental study of exfoliated graphite solar thermal coating on a receiver with a Scheffler dish and latent heat storage of desalination. Solar Energy, 151: 129–45.

- **Dafle, V.R. and N.N. Shinde. 2012.** Design, development and performance evaluation of concentrating monoaxial Scheffler technology for water heating and low temperature industrial steam application. IJERA, 6: 848–52.

- **Dincer, I. 1999.** Evaluation and selection of energy storage systems for solar thermal applications. International Journal of Energy Research, 23: 1017–28.

- **Duffie, J., Beckman, W., 2006.** Solar engineering of thermal processes, 3rd edition, John Wiley & Sons, Inc.Hoboken, New Jersey ISBN -13 978-0-471-69867-8

- **EESI. 2011.** Solar thermal energy for industrial uses. Environmental and Energy Study Institute (ESSI), Issue Brief.

- F**AO. 2009.** How to feed the world in 2050. Rome: FAO. Available at: www.fao.org/fileadmin/templates/wsfs/docs/expert_paper/How_to_Feed_the_World_in_2050.pdf.

- **FAO. 2011.** Energy-smart food for people and climate. Issue Paper: Food and Agriculture Organization of the United Nations (FAO). In Rome, p.78 (also available at: www.fao.org/docrep/014/i2454e/i2454e00.pdf)

- **FAO. 2013.** Food wastage footprint: impacts on natural resources. Rome. (also available at www.fao.org/3/i3347e/i3347e.pdf

- **Farid, M.M., A.M. Khudhair, S.A.K. Razack, and S.A. Al-Hallaj S. 2004.** A review on phase change energy storage: materials and applications. Energy Conversion and Management. 45:1597-615.

- **Garg, H.P., and J. Prakash. 2006.** Solar energy for industrial process heat. Solar energy fundamentals and applications. New Delhi: Tata McGraw-Hill.

- **Höök, M. and T. Xu.2013.** Depletion of fossil fuels and anthropogenic climate change – a review. Energy Policy, 52: 797–809.

- **International Energy Agency (IEA). 2008.** Process Heat Collectors: State of the Art within Task 33/ IV. Available at: www.iea-shc.org/publications/downloads/task33-Process_Heat_Collectors.pdf

- **International Energy Agency (IEA). 2011.** Solar heating and cooling program. solar heat worldwide: markets and contribution to the energy supply 2009 (available at: www.iea-shc.org/publications/downloads/Solar_Heat_Worldwide-2011.pdf)

- **Jaisankar, S., J.A. Ananth, S. Thulasi, S.T. Jayasuthakar, and S. Narayanan. 2011.** A comprehensive review on solar water heaters. Renewable and Sustainable Energy Reviews, 15(6): 3045–3050.

- **Jegadheeswaran, S., S.D. Pohekar, and T. Kousksou. 2010.** Energy based performance evaluation of latent heat thermal storage system: a review. Renewable and Sustainable Energy Reviews, 14: 2580–95.

- **Jannot, Yves, 2003.** Cours de transert thermique. Available at: www.econologie.com/file/technologie_energie/Transferts_thermiques_cours.pdf

- **Kalogirou, S., 2003.** Potential of solar industrial process heat applications. Applied Energy, 76: 337–61

- **Kamboj, V.K. and A.J. Yadav. 2017.** Experimental investigation of solar powered coffee maker based on Scheffler reflector. In: 4th International Conference on Recent Development in Engineering Science, Humanities and Management.

- **Kenisarin, M. and K. Mahkamov. 2007.** Solar energy storage using phase change materials. Renew Sustain Energy Rev., 11: 1913–65.

- **Kumar, N.S. and K.S. Reddy. 2007.** Numerical investigation of natural convection heat loss in modified cavity receiver for fuzzy focal solar dish concentrator. Solar Energy, 81: 846–55.

- **Lauterbach, C., B. Schmitt, U. Jordan, and K. Vajen. 2012.** The potential of solar heat for industrial processes in Germany. Renewable and Sustainable Energy Reviews. 16: 5121–30.

- **Le Quéré, C., R.M. Andrew, J.G. Canadell, S. Sitch, J.I. Korsbakken, G.P Peters, and R.F. Keeling. 2016.** Global carbon budget 2016. Earth System Science Data, 8(2): 605.

- **Mussard, M. 2013.** A solar concentrator with heat storage and self-circulating liquid. Ph.D. thesis, Faculty of Engineering Science and Technology, Norwegian University of Science and Technology, Trondheim, 2013.

- **Neftel, A., E. Moor, H. Oeschger, and B. Stauffer. 1985.** Evidence from polar ice cores for the increase in atmospheric CO_2 in the past two centuries. Nature, 315: 45–7.

- **Oparaku, O.U. and O.C. Iloeje. 1991.** Design considerations for a photovoltaic-powered water-pumping facility in a rural village near Nsukka. Nigerian Journal of Renewable Energy. 10: 64–69.

- **Panchal, H., J. Patel, K. Parmar and M. Patel. 2018.** Different applications of Scheffler reflector for renewable energy: a comprehensive review. International Journal of Ambient Energy. doi: 10.1080/01430750.2018.1472655.

- **Patil, R., G.K. Awari, and M.P. Singh. 2011.** Experimental analysis of Scheffler reflector water heater. Therm Sci.,15(3): 599–604.

- **Quaschning, V. 2010.** Renewable energy and climate change (1st ed.). John Wiley & Sons Ltd Chichester, ISBN: 978-0-470-74707-0.

- **REN21. 2017.** Renewables 2017 Global status report. ISBN: 978-3-9818107-6-9. Paris, REN21 Secretariat.
- **Rezaei, M. and B. Liu. 2017.** Food loss and waste in the food supply chain. Feature Article in NUTFRUIT: 26–27.
- **Ruelas, J., J. Palomerous, and G. Pando. 2015.** Absorber design for a Scheffler type solar concentrator. Applied Energy. 154: 35-39.
- **Scheffler, W., S. Bruecke, and G. von-Werdenbergstr. 2006.** Development of a solar crematorium. In: Proceedings of Sixth International Conference on Solar Cooker. Granada, Spain.
- **Sharma, A, V.V. Tyagi, C.R. Chen, and D. Buddhi. 2009**. Review on thermal energy storage with phase change materials and applications. Renew Sust. Energ. Rev., 13: 318–45.
- **Sharma, S.D. and K. Sagara. 2005**. Latent heat storage materials and systems: a review. Int. J. Green Energy. 2:1-56.
- **Sudhir, C.V. and S.S. Feroz. 2016.** Potential of 16 m^2 solar Scheffler reflectors for thermal applications: experimental investigation. International Journal of Advances in Engineering and Technology, 4(2): 42–46.
- **Tverberg, G. 2018.** World energy consumption to 2017 BP fossil fuel other (available at: https://ourfiniteworld.com/2018/06/22/eight-insights-based-on-december-2017-energy-data/world-energy-consumption-to-2017-bp-fossil-fuel-other/).
- **World Resources Institute. 2017.** Global manmade greenhouse gas emissions by sector (available at: www.c2es.org/content/international-emissions/).
- **Zalba, B., J.M. Marin, L.F. Cabeza, and H. Mehling. 2003.** Review on thermal energy storage with phase change: materials, heat transfer analysis and applications. Appl. Therm. Eng., 23: 251–83.

APPENDICES

Appendix-A

FRAGOLTHERM© Q-32-N			METHOD
Density @ 20°C	[kg/m³]	871	
Viscosity @ 40°C	[mm²/s]	31,00	
Viscosity @ 100°C	[mm²/s]	5,40	
Pourpoint	[°C]	–12	ISO 3016
Flashpoint	[°C]	220	ISO 2592
Boiling point @ 1013 mbar	[°C]	360	DIN 51356
Film temperature max.	[°C]	340	
Bulk temperature max.	[°C]	320	
Water hazard class	[–]	1	
Dangerous goods according to IATA/IMDG/ADR	[–]	no	

Appendix-B

SUBSTANZ	LIEFERANT	SCHMELZ-TEMPE-RATUR [°C]	SCHMELZ-ENTHALPIE [KJ/KG]	WÄRMELEIT-FÄHIGKEIT [W/M K]	DICHTE [KG/M³]	SPEICHER-DICHTE [K WH/M³]
Erythritol	Reformhaus	118	339,8	0,326	1300	123,76
Isomalt	Südzucker	147	170	n.a.	n.a.	
Maltitol	Roquette	145	173	n.a.	n.a.	
Mannitol	Roquette	166,85	336,8	0,5	1620	152,86
KN03/NaNO3 Eutekt.	BASF	223	105	0,8	2150	63,21
Wasser	Wasserhahn	0	335	2,4	1000	93,8

Appendix-C

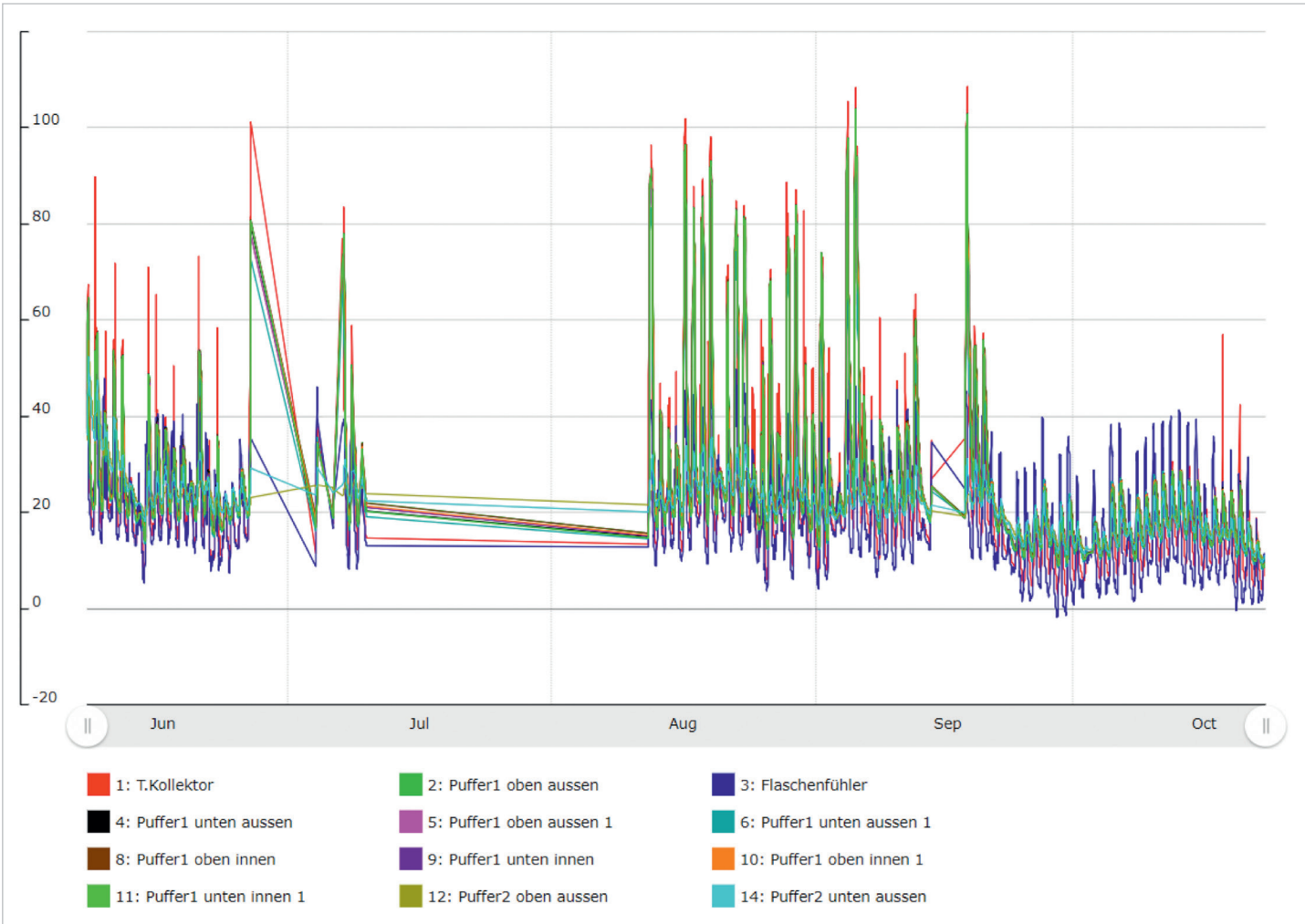
100
80
60
40
20
0
-20
Jun
Jul
Aug
Sep
Oct
1: T.Kollektor
2: Puffer1 oben aussen
3: Flaschenfühler
4: Puffer1 unten aussen
5: Puffer1 oben aussen 1
6: Puffer1 unten aussen 1
8: Puffer1 oben innen
9: Puffer1 unten innen
10: Puffer1 oben innen 1
11: Puffer1 unten innen 1
12: Puffer2 oben aussen
14: Puffer2 unten aussen

Appendix-D

Positions of Scheffler reflector during the experiment on September 5, 2018:


10:21 AM


11:21 AM


12:35 AM


01:05 PM


01:30 PM


02:00 PM


02:30 PM


03:30 PM


04:00 PM


05:00 PM


05:30 PM


06:00 PM

ICDD Working Paper Series

- **Vol. 1: Webster, Edward:** Work and Economic Security in the 21st century. What Can We Learn from Ela Bhatt?, 17 pages

- **Vol. 2: Hagmann, Jonas:** Opportunities and Constraints of Peri-urban Buffalo and Dairy Cattle Systems in Faisalabad, Punjab, Paki stan, 48 pages

- **Vol. 3: Marchetti, Sabrina:** Together? On the Not-so-easy Relationship between Italian Labour Organisations and Migrant Domestic Workers' Groups, 23 pages

- **Vol. 4: Sinaga, Hariati / Scherrer, Christoph:** Core Labor Rights: Competitive Pressures and Non-Compliance, 29 pages

- **Vol. 5: Burchardt, Hans-Jürgen / Weinmann, Nico:** Social Inequality and Social Policy outside the OECD: A New Research Perspective on Latin America, 39 pages

- **Vol. 6: Beck, Stefan:** Sozial verantwortliche Beschaffung von Informationstechnik. Socially Responsible Public Procurement of Information Technology, ISBN 978-3-944090-08-5, 40 pages

- **Vol. 7: Aufderheide, Mareike / Voigts, Clemens / Hülsebusch, Christian / Kaufmann, Brigitte:** Decent Work? How Self-employed Pastoralists and Employed Herders on Ranches Perceive their Working Conditions, ISBN 978-3-944090-05-4, 28 pages

- **Vol. 8: Bhattacharjee, Manojit / Rajeev, Meenakshi:** Credit Exclusion of the Poor: A Study of Cultivator Households in India, ISBN 978-3-944090-09-2, 22 pages

- **Vol. 9: Younas, Muhammad:** The Dairy Value Chain: A Promoter of Development and Employment in Pakistan, ISBN 978-3-944090-06-1, 22 pages

- **Vol. 10: Erbach, Juliane:** The Decency of Women's Working Conditions in Peri-urban Buffalo Production Systems in the District Faisalabad, Punjab, Pakistan, kassel university press, ISBN 978-3-86219-692-0, 45 pages

- **Vol. 11: Schützhofer, Timm B.:** Can Decent Work and Export Oriented Growth Strategies Go Together? Lessons from Nicaragua's Export Processing Zones, kassel university press, ISBN 978-3-86219-810-8, 52 pages

- **Vol. 12: Bhattacharya, Tulika / Rajeev, Meenakshi:** Identifying Employment Creating Sectors in India: An Analysis of Input-Output Linkages, kassel university press, ISBN 978-3-86219-852-8, 28 pages

- **Vol. 13: Withanachchi, Sisira Saddhamangala / Houdret, Annabelle / Nergui, Soninkhishig / Ejarque i Gonzalez, Elisabet / Tsogtbayar, Ankhbold / Ploeger, Angelika:** (Re) configuration of Water Resources Management in Mongolia: A Critical Geopolitical Analysis, kassel university press, ISBN 978-3-86219-860-3, 42 pages

- **Vol. 14: Gordana Kranjac-Berisavljevic:** Transformations of traditional landuse systems and their effects on development opportunities and people's livelihoods, kassel university press, ISBN 978-3-7376-0032–3, 24 pages

- **Vol. 15: Meenakshi Rajeev, Manojit Bhattacharjee, B P Vani:** Crop Insurance and Risk Mitigation: Experiences from India, kassel university press, ISBN 978-3-7376-0066-8, 34 pages

- **Vol. 16: William Baah-Boateng (PhD):** Economic growth and employment generation nexus: Insight from Ghana, kassel university press, ISBN 978-3-7376-0068-2, 24 pages

- **Vol. 17: Madhushree Sekher / Suchandrima Chakraborty:** Politics of public policies in India: Explaining the institutional internalization of inequality in policy legislation, kassel university press, ISBN 978-3-7376-0248-8, 38 pages

- **Vol. 18: Tripti Kumari:** Microfinance through Women Self-Help Groups (SHGs) for Grass-root level Empowerment: An Empirical study of Varanasi, Uttar Pradesh, India, kassel university press, ISBN 978-3-7376-0256-3, 25 pages

- **Vol. 19: Meenakshi Rajeev, B.P. Vani and Veerashekharappa:** Self-help groups for India's financial inclusion: Do effective costs of borrowing limit their operation?, kassel university press, ISBN 978-3-7376-0384-3, 26 pages

- **Vol. 20: Praveen Jha:** India's Macroeconomic Policy Regime and Challenges of Employment: Some Reflections on the Manufacturing Sector, kassel university press, ISBN 978-3-7376-0440-6, 56 pages

- **Vol. 21: Meenakshi Rajeev, Pranav Nagendran:** Decency of primary occupations in the Indian fishing industry, kassel university press, ISBN 978-3-7376-0452-9, 35 pages

- **Vol. 22: Dr. Tolga Tören:** Documentation Report: Syrian Refugees in the Turkish Labour Market, kassel university press, ISBN 978-3-7376-0450-5, 67 pages

- **Vol. 23: Dr. Tulika Bhattacharya:** Farmers in Peri-Urban Regions: Socio-Economic Changes and Access to Finance Study for Indian Economy, ISBN 978-3-7376-0576-2, 51 pages

- **Vol. 24: Akua Opokua Britwum, Angela Dziedzom Akorsu, Loretta Baidoo**: Women's empowerment for sustainable rural livelihoods: Voices from selected communities in Ghana., ISBN 978-3-7376-0630-1, 33 pages

- **Vol. 25: Christa Wichterich:** Care Extractivism and the Reconfiguration of Social Reproduction in Post-Fordist Economies, ISBN 978-3-7376-0632-5, 27 pages

The Global ICDD Network

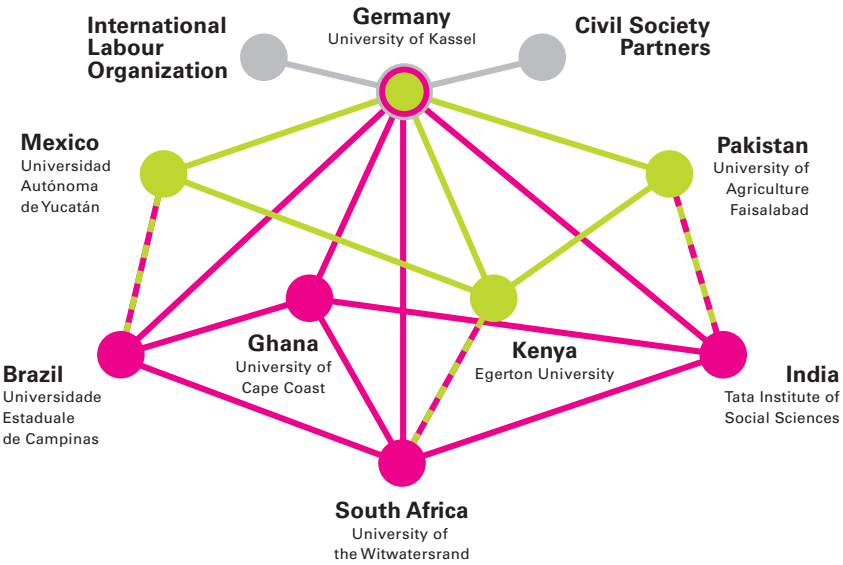

International Center for
Development and Decent Work
University of Kassel, Germany
Phone: + 49 (0) 561 804-7399
E-Mail: felmeden@icdd.uni-kassel.de

With financial support from the

Federal Ministry for Economic Cooperation and Development

DAAD Deutscher Akademischer Austauschdienst German Academic Exchange Service

UNIKASSEL VERSITÄT

exceed EXCELLENCE CENTERS FOR EXCHANGE AND DEVELOPMENT

▶▶▶ www.icdd.uni-kassel.de